Title

REACTIONS OF He3 WITH LIGHT ELEMENTS: APPLICATIONS TO ACTIVATION ANALYSIS

Permalink

https://escholarship.org/uc/item/89n83375

Author

Mahony, John D.

Publication Date

1965

University of California

Ernest O. Lawrence Radiation Laboratory

REACTIONS OF He^3 WITH LIGHT ELEMENTS: APPLICATIONS TO ACTIVATION ANALYSIS

Berkeley, California

Research and Development

UCRL-11780

UNIVERSITY OF CALIFORNIA

Lawrence Radiation Laboratory
Berkeley, California

AEC Contract No. W-7405-eng-48

REACTIONS OF He^3 WITH LIGHT ELEMENTS: APPLICATIONS TO ACTIVATION ANALYSIS

John D. Mahony

(Ph.D. Thesis)

January 1965

REACTIONS OF He^3 WITH LIGHT ELEMENTS: APPLICATIONS TO ACTIVATION ANALYSIS

Contents

Appendices

REACTIONS OF He^3 WITH LIGHT ELEMENTS: APPLICATIONS TO ACTIVATION ANALYSIS

John D. Mahony

Lawrence Radiation Laboratory
University of California
Berkeley, California

January 1965

ABSTRACT

A simple, rapid technique of analyzing for carbon, oxygen, and fluorine, individually and simultaneously by He^3 activation is presented. This method, which can easily be extended to other elements, is capable of analyses at the ppb level or even less in some cases and an ultimate accuracy of 5%. Milligram amounts of total sample are sufficient and are not destroyed in the analysis. The advantages of this technique with especial reference to energetics, versatility and the elimination of interferences are discussed and compared to those of other charged-particle and neutron-activation analysis procedures.

The excitation functions for the production of F^{18} from O^{16}, C^{11} and N^{13} from C^{12}, and F^{18} from F^{19} by He^3 reactions for the energy range, 0 to 31 MeV have been determined and are discussed with particular application to activation analysis.

An absolute analysis for oxygen in thorium was performed; simultaneous absolute analyses of gold, silicon, Mylar, and polyethylene for carbon and oxygen, and Teflon for carbon and fluorine are described. Results of analyses by the relative method for oxygen in thorium, beryllium, niobium, and lead are also reported.

Although the Berkeley Hilac was used for the work described, a small cyclotron is shown to be quite adequate for extensive He^3 activation analysis. The specifications of such an accelerator are given.

I. INTRODUCTION

The rather exotic identification of He^3 as both a stable nuclide and a potential projectile in nuclear reactions was reported by Alvarez and Cornog in 1939,[1] who used the 60-inch Crocker cyclotron as a mass spectrograph. The importance of investigating He^3 reactions was recognized by Barkas[2] in the same year. However, the availability of He^3 was extremely limited and eleven years later the gas was still prohibitively priced at $250 per ml at S.T.P., about 10 million times that of gold. By 1959 the price had dropped to $1.50 per ml; the current price is $0.10 per ml. Not surprisingly experimental studies of He^3 reactions were somewhat rare until after 1950.

By 1959 considerable material on He^3 reactions had appeared in the literature and a general survey of this field was published by Bromley and Almquist.[3] From this report it was quite clear that the first expectations as to the value of such reaction studies were more than justified. He^3 projectiles were found to be useful tools in the elucidation of nuclear-reaction mechanisms. In addition He^3 reactions found application in nuclear spectroscopy especially for obtaining final nuclei at high excitation from low-energy bombardment, for isobaric multiplet studies of the charge independence of nuclear forces, for shell structure investigations using the (He^3,n) reaction, which adds two protons to the target nucleus, and finally for providing information on nucleon clustering. Most of this work, however, was confined to low energy (less than 5 MeV) He^3 ions and reactions involving the light elements.

In an effort to study the reactions of He^3 ions at higher energies, Markowitz and Hall[4] in 1958 obtained beams of He^3 ions accelerated to a maximum energy of 17.7 MeV at the Crocker 60-inch cyclotron and to a maximum energy of 31.2 MeV at the heavy-ion linear accelerator (HILAC). Using the stacked-foil technique, they obtained excitation functions for the following reactions $Al^{27}(He^3,2\alpha)Na^{22}$, $Al^{27}(He^3,3\alpha)F^{18}$,

$Al^{27}(He^3,2p)Na^{24}$, and $Be^9(He^3,n)C^{11}$ over the range 0 to 31.2-MeV He^3 ions. In addition they obtained preliminary excitation functions for the reactions $C^{12}(He^3,\alpha)C^{11}$, and $C^{12}(He^3,d \text{ and } np)N^{13}$ as well as $O^{16}(He^3,p)F^{18} + O^{16}(He^3,n)Ne^{18} \xrightarrow[1.5\text{ sec}]{\beta+} F^{18}$.

The data for the excitation function for the reaction $Al^{27}(He^3,3\alpha)F^{18}$ ($Q = -10.4$)MeV) yielded an appreciable cross section for the formation of F^{18} far below the threshold for its production from aluminum (Fig. 1). This anomaly was attributed to the reaction of He^3 with oxygen on the surface of the aluminum. The possibility of He^3 activation as a method of analysis for oxygen and other light elements was thus suggested.

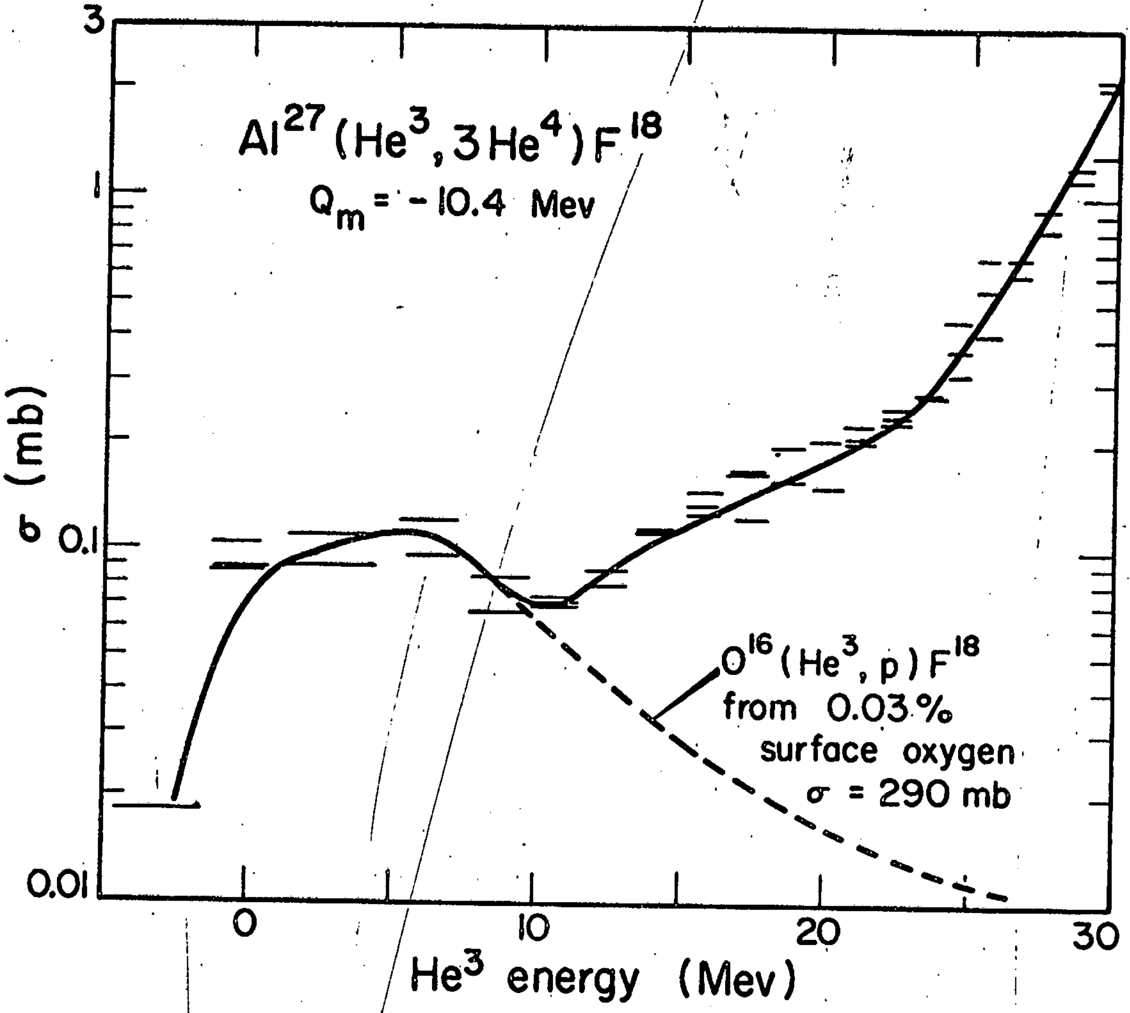

MU-16577

Fig. 1. Excitation function for production of F^{18} from Al^{27} by He^3 bombardment.

II. ACTIVATION ANALYSIS AND He^3 REACTIONS

The technique of analysis by nuclear activation is nearly as old as the discovery of artificial radioactivity itself. In January 1934, I. Curie and F. Joliot prepared N^{13} and P^{30} from the alpha particle bombardment of boron and aluminum. In 1936, the first activation analysis was carried out by Hevesy and Levi[5] who used thermal neutrons from a radon-beryllium source to determine the concentration of dysprosium in yttrium. Charged particles were first used in activation analysis by Seaborg and Livingood[6] in 1938 when they used deuterons to determine the presence of trace quantities of gallium in iron.

From these beginnings the expansion of scientific investigation and knowledge in this field has followed the traditional exponential pattern. After 1949 review articles have appeared with increasing frequency.[7,8,9,10] By 1955 activation analysis was an established laboratory technique and in addition to general review articles[11,12,13,14] many papers discussing special applications such as ion exchange,[15] gamma spectrometry,[16] and dating of minerals[17] were published. After 1955 many excellent review articles appeared, only a few of which can be cited here. Those of Leddicotte,[18] Jenkins and Smales,[19] and Taylor and Havens[20] are noteworthy. In addition those of Meinke,[21,22] Gibbons,[23] and Koch[24] provide not only an exhaustive coverage of the field but also extensive bibliographies. The theoretical and practical aspects of radioactivation analysis are discussed extensively in books by Bowen and Gibbons[25] and Albert.[26] Further special applications of activation analysis to the measurement of such physical properties as particle size[27] and surface composition[28] were also reported. The article of Odeblad,[29] which considers in detail the basic principles of charged particle activation analysis, is to be noted. More specific to our work is a review of nuclear methods of oxygen analysis by Bate.[30]

Neutron activation has been used in the analysis for oxygen, fluorine, and nitrogen; photon[31] and charged particle[33,34,36,37,38] reactions have been used for these elements, and, in addition, for carbon[31,32,35] where neutron activation is not feasible. Up to 1960 only[*] alpha particles,[33,34] deuterons,[32,35,36] protons[37,38] were employed as incident particles. Each of these particles presented certain difficulties, while He^3 ions offered distinct and contrasting advantages.

The binding energy of the He^4 nucleus is 28.3 MeV; the binding energy of the He^3 nucleus is only 7.7 MeV, thus many of the simple nuclear reactions of the mass-3 isotopes are exoergic while similar reactions of the alpha particle need considerable incident energy. The following reactions and their Q-values are illustrative for the case of oxygen analysis.

$O^{16}(He^3,p)F^{18}$	$Q = +2.0$ MeV
$O^{16}(He^4,d)F^{18}$	$Q = -16.3$ MeV
$O^{16}(He^3,\alpha)O^{15}$	$Q = +4.9$ MeV
$O^{16}(He^4,\alpha n)O^{15}$	$Q = -15.7$ MeV

Thus to analyze for oxygen by the detection of either 109.7-min F^{18} or 124-sec O^{15}, alpha particles of almost 20-MeV laboratory energy would be required. He^3 particles require only sufficient energy to overcome the Coulomb barrier, which is about 4 MeV for O^{16} and increases to about 8 MeV for Ca^{40}. The Coulomb barrier for He^3 ions as a function of atomic number is shown in Fig. 2. The capability of He^3 ions to produce nuclear reactions at low energies eliminates interfering radioactivities considerably. Thus, for oxgyen analysis, 5-MeV He^3 particles would be sufficient and radioactivities from all elements heavier than sodium are

---

[*] The use of tritium obtained from the $Li^6(n,\alpha)t$ reaction, as the incident particle in oxygen analysis was reported by Osmond and Smales,[39] however, the limitations of low effective cross section (0.5 mb) and necessity of chemical separation limit its applications. (The direct acceleration of tritium, a radioactive projectile, would present considerable complications to possible use in activation analysis.)

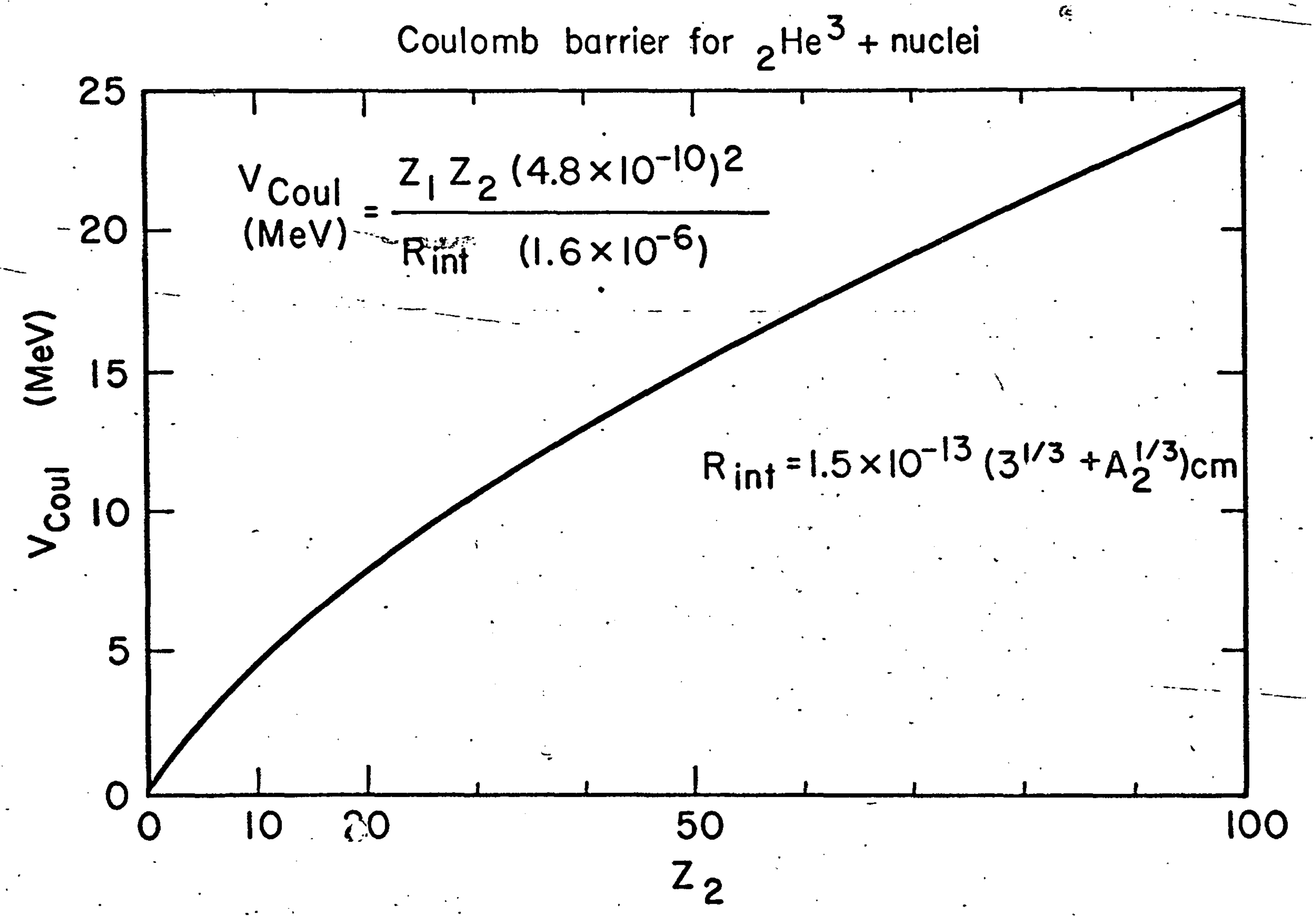

MU-32162

Fig. 2. Coulomb barrier for He^3 ions as a function of atomic number.

excluded. Analysis by alpha-particle bombardment would require an incident energy of about 25 MeV, at which virtually no element is eliminated.

The deuteron, which has a binding energy of 2.2 MeV, will produce exoergic (d,p) reactions and some exoergic (d,n,) reactions. The high neutron background, surrounding deuteron accelerators, induces (n,γ) reactions that give the same product as (d,p) reactions thus complicating the analysis. No such complication is present with the use of He^3. Further, detection of the annihilation radiation from positron decay is quite convenient especially in the presence of other radioactivity. The products of (d,p) or (n,γ) reactions, however, usually decay by negatron emission whereas those of He^3, being proton rich, are positron emitters.

Although the Coulomb barrier for protons is lower than that for He^3 particles, most proton reactions are considerably endoergic. In addition most low-energy protons induce only (p,n) reactions, thus sharply limiting the number of products that can be detected. For example, in the case of oxygen, O^{18} must be used in proton activation; the low abundance of the mass-18 isotope greatly limits the sensitivity.[40]

Finally, because many of the He^3 reaction products are so neutron-deficient and relatively short-lived, they quickly decay to form a radioactive daughter of convenient half-life rather than a stable nuclide. The measured cross section is thus enhanced because there are two reactions leading to the same product. This enhancement cannot, in most cases, take place for low-energy proton, deuteron, or alpha irradiations.

The He^3 ion, like other charged nuclear particles, has a relatively short range (compared to neutrons) e.g., about 0.017 inches (125 mg/cm^2) in aluminum for a 30-MeV He^3 particle. Surface etching or grinding may be employed, however, to reach deeper portions of the bulk material. The same procedures would be necessary for the analysis of substances that react with or absorb oxygen or carbon dioxide from the air. On the other hand, by controlling the depth of penetration and successive surface removal and irradiation, a profile rather than a simple bulk analysis is possible.

The work described in this report represents an investigation of the reactions of He^3 with oxygen, carbon, fluorine, and nitrogen, primarily from the point of view of application to activation analysis. Because it was the intent to develop the principles and breadth of application of this new analytical procedure, the analyzed systems mentioned in this research are by no means developed, at this stage, to the full precision and accuracy possible. Additional discussion of this technique with respect to sensitivity, depth of penetration, sample handling, interferences and energetics is contained in the paper of Markowitz and Mahony.[41]

III. MATHEMATICAL RELATIONSHIPS

A. Cross-Section and Absolute-Analysis Calculations

Koch[42] defines activation analysis as, "a method of measuring concentrations of constituents in a given sample by measuring the characteristic radiations emitted by the radioactive nuclides resulting from selected nuclear transformations." For an accelerator bombardment the mathematical relationship between the disintegration rate of an induced nuclide and the amount of the constituent in a thin target approximation is given by

$$D_o = nI\sigma \left[1 - \exp(-0.693\tau/T_{1/2})\right] \quad , \qquad (1)$$

where

D_o = disintegration rate at the end of bombardment of the nuclide produced from the constituent whose concentration is to be determined, in dis/min,

n = number of target atoms per cm^2 of the nuclide being determined,

I = average beam intensity, in incident ions per min,

σ = cross section for the reaction, in cm^2 per target atom-incident ion,

τ = length of bombardment, in minutes,

$T_{1/2}$ = half-life of the product nuclide, in minutes.

The intensity of charged particles in an accelerated beam is usually measured in units of the beam current, in microamperes, striking the target. Beam current in μA is converted into $He^3(++)$ ions by a factor based on the unit positive or negative charge (1.602 × 10^{-19} C). Thus

$$1\ \mu A \text{ of } He^3(++) = 1.873 \times 10^{14}\ He^3(++)/\text{min}.$$

The disintegration rate, D_o, at the end of bombardment is determined by the relationship

$$D_o = A_o/\mathrm{ODC} \quad , \qquad (2)$$

where

A_o = product activity, in counts/min, at the end of bombardment, and

ODC = over-all detection coefficient, defined as A_o/D_o.

The ODC thus includes decay scheme, counter efficiency, geometry, absorption, scattering, and any other counter factors. It is measured independently, or estimated, for each detection arrangement used.

The preceding relationships may be used to obtain cross sections as a function of incident-particle bombarding energy if the number of target nuclei per cm^2, n, is known. Once the cross section for the production of a particular nuclide is measured, n may be determined directly.

The mass per cm^2, m, of the target nuclei can easily be determined from A, the mass number, Avogadro's number, and n by the formula

$$m = nA/6.025 \times 10^{23} \quad . \qquad (3)$$

If an absolute analysis is to be performed, all parameters in Eq. (1) except n must be known or determined during the experiment.

B. Relative-Analysis Calculations

A relative analysis may be carried out by bombarding and counting a sample and standard under identical, or nearly identical conditions. The ratio of A_o for the unknown sample, x, to that for the standard, s, using Eqs. (1) and (2) is

$$\frac{A_{ox}}{A_{os}} = \frac{n_x\ \sigma_x\ I_x\ (ODC)_x\ [1 - \exp(-0.693\tau_x/T_{1/2})]}{n_s\ \sigma_s\ I_s\ (ODC)_s\ [1 - \exp(-0.693\tau_s/T_{1/2})]}\ , \qquad (4)$$

where n_x and n_s are the number of target atoms per cm^2 available to the beam in the unknown and standard matrices respectively, σ_x and σ_s the production cross sections for the radioactive nuclide to be counted in unknown and standard, (σ is energy-variant), I_x and I_s the average beam intensity received by unknown and standard, $(ODC)_x$ and $(ODC)_s$ the over-all detection coefficient for unknown and standard, and τ_x and τ_s the length of bombardment for unknown and standard. If the standard and unknown are counted under identical conditions $(ODC)_x$ and $(ODC)_s$ will be the same. If this is not possible then a correction must be applied.

When a thin-sample, thin-standard procedure is used in which both are bombarded in the same beam (see Fig. 10a), Eq. (4) reduces to

$$\frac{A_{o_x}}{A_{o_s}} = \frac{n_x}{n_s}\ , \qquad (5)$$

when corrections are applied for differences in σ_x and σ_s.

The mass per cm^2, m_x, of the target nuclei in the unknown is, from Eq. (3)

$$m_x = \frac{n_x A}{N} \text{ grams per } cm^2\ , \qquad (6)$$

where A is the again mass number of nuclide being determined and N is Avogadro's number.

When a thin-sample, thin-standard procedure is used in successive irradiations (see Fig. 10b), Eq. (4) again reduces to Eq. (5), however, in addition to a possible correction of σ_x and σ_s if unknown and standard have unequal differential energy-loss functions, corrections for differences in I_x and I_s, as well as τ_x and τ_s may have to be applied. Equation (6) is again used to calculate m_x.

When a thick sample, thin standard procedure (see Fig. 10c) is employed only a single bombardment is necessary. Equations (5) and (6) are used with the appropriate correction for σ_x and σ_s. In this case, because the sample is a "thick target," σ_x is an average cross-section over the effective range of the beam. Only the mass per cm^2 of the unknown matrix in this range is used in percentage calculations.

When a thick-sample, thick standard procedure (see Fig. 10d) must be employed, two successive irradiations are required. Equations (5) and (6) are used; corrections for σ_x and σ_s, I_x and I_s, and τ_x and τ_s will usually be necessary.

Usually only a portion of the cross-sectional area of the sample will be illuminated by the beam. This is the case in all of the above relationships. When the sample is extremely small, however, it will be necessary to adopt an arrangement wherein the sample is completely immersed in the beam. In such a case the ratio of A_o for the unknown sample to A_o for the standard using Eqs. (1) and (2) is

$$\frac{A_{o_x}}{A_{o_s}} = \frac{n'_x\ \sigma_x\ (I/a)\ (ODC)_x\ [1 - \exp(-0.693\tau_x/T_{1/2})]}{n'_s\ \sigma_s\ (I/a)\ (ODC)_s\ [1 - \exp(-0.693\ {}_s/T_{1/2})]} \qquad (7)$$

where n'_x and n'_s are the number of target atoms available to the beam in the unknown and standard matrices respectively and a is the cross-sectional area of the beam. If the beam is completely stopped in each sample, the mass, m, actually bombarded by the He^3 ions is

$$m = Rs \qquad (8)$$

where R is the range in mg/cm^2, of the He^3 ions in the sample at the energy used and p is the surface area os the sample. If f is the weight fraction of the target nuclide in the sample Eq. (3) becomes

$$m = nA/fN \qquad (9)$$

where N is Avogadro's number. Combining Eqs. (5) and (6) we obtain

$$n = pfNR/A \quad . \qquad (10)$$

when Eq. (7) is substituted into Eq. (4), assuming the same beam is used in the bombardment of standard and unknown and the product activities are counted under identical conditions, we obtain for the weight fraction of the nuclide being determined

$$f_x = \frac{A_{o_x} R_s p_s f_s}{A_{o_s} R_x p_x} \quad . \qquad (11)$$

In practice the cross section σ is determined for each particular reaction as a function of energy by bombardment of targets of known composition. While this measurement is necessary only for an absolute analysis it is quite useful in relative analyses to establish feasibility, as well as optimum bombarding energy for efficient detection and minimization of interferences.

IV. REACTION STUDIES AND EXCITATION FUNCTIONS

A. General Experimental Procedures

In this section we first describe the general procedures used to determine the excitation functions for the reactions

$$O^{16}(He^3,p)F^{18} + O^{16}(He^3,n)Ne^{18} \xrightarrow[1.5\ \mathrm{sec}]{\beta+} F^{18}$$

$$C^{12}(He^3,\alpha)C^{11}$$

$$C^{12}(He^3,np)N^{13} + C^{12}(He^3,d)N^{13}$$

$$F^{19}(He^3,\alpha)F^{18}.$$

We then consider the individual reactions and the experimental details which are specific to each excitation function.

1. He^3 Beam

The Berkeley heavy ion linear accelerator (HILAC) was used in all experiments. Mixtures of 2 to 4% He^3 in He^4 gas proved a convenient and economical ion source. The Hilac accelerated single-charged He^3, which was stripped to form $He^3(++)$ ions, then bent magnetically and collimated through a 3/8-in. aperture before impinging on the target. The maximum beam energy[43] was 31.2 ± 0.6 MeV.

2. The Target

The stacked-foil technique was employed in the determination of the excitation functions. Suitable plastic foils were used as sources of the target nuclei. Aluminum and gold foils were used in the stack to degrade the beam and promote heat transfer from the plastics. Both the plastic and metal foils were cut with a precision punch, the plastics 11/16 to 13/16-in. diameter, the metal 1-in. diameter. Sufficient plastic and degrader foils were used in each stack so that the beam was completely attenuated in the target. Whenever excess beam intensity caused the plastic foils to be burned or discolored, the experiment was discarded. Protector foils were included to prevent the plastic foils from being contaminated with recoiling nuclei produced in the metal foils.

The approximation was usually made that any product nuclei recoiling out of the plastic was compensated by recoil gain from the adjacent foil. In several experiments the plastic foil was sandwiched between two foils from which the product nuclide could not be formed. The three foils were counted separately and the total activity from the nuclei being measured was compared with that obtained by the approximate method. No appreciable difference was observed except when the excitation function was steeply sloped. In these sections the three-foil procedure was used.

All foils were cleaned with appropriate solvents and weighed before mounting in a conventional water cooled, tag target assembly.

The problem of recoil gas-loss from the irradiated foils is treated in Section IV, E, Estimation of Errors.

3. Range-Energy Relations

The energy of the He^3 beam at the appropriate foil position in the stack is determined from range-energy relations. For He^3 these relations must be calculated since experimental values are not available. When reliable empirical proton or alpha particle ranges for a given material are available it is possible to calculate the range-energy relations for He^3 in that material from the formulas[44]

$$R_{He^3}(3E) = 3/4\ R_p(E) \quad \text{or}$$

$$R_{He^3}(3E) = 3/4\ R_\alpha(4E) \quad .$$

Otherwise it is necessary to compute the ranges by numerical integration of the inverse kinetic-energy loss function.

The range-energy relations for He^3 in aluminum are available from several sources. Rich and Madey[45] calculated the ranges from the proton data of Smith.[46] Bromley and Almquist[3] compiled their ranges from the stopping cross section data of Whaling.[47] Markowitz has calculated this relation from the experimental proton ranges of Bichsel.[48]

Theoretical computations have recently been published by Demildt[49] and by Williamson and Boujot.[50] The ranges of Demildt and of Rich and Madey are in very close agreement. Those of Markowitz and of Williamson and Boujot are also in close agreement but are about 2% higher than the values of Demildt and of Rich and Madey. The ranges compiled by Bromley and Almquist are 5% higher than those of Demildt and of Rich and Madey. With respect to the rate of energy loss, however, the agreement is considerably better since the variously reported range-energy relations are nearly parallel when log range is plotted vs. log energy.

In our calculations we have used for He^3 in aluminum the ranges of Markowitz. They are based on the most recent experimental data. In addition these values are in close agreement with the theoretical analysis of Williamson and Boujot.

For the reported ranges of He^3 in gold there is not the 5% overall agreement which exists for aluminum. For example at 25 MeV the range of He^3 in gold is calculated to be 170 mg/cm^2 on the basis of proton ranges compiled by Rybakov[51] and reported in Nuclear Data Tables.[52] Bromley and Almquist give 193 mg/cm^2 and Williamson and Boujot, 218 mg/cm^2 (Demildt reports 201 mg/cm^2 as the range of a 25 MeV He^3 ion in platinum). Since, however, the various range curves are nearly parallel above 10 MeV when log range is plotted against log energy, the respective energy losses per mg/cm^2 are not significantly different for He^3 energies between 31 and 10 MeV. The use of gold degrader or catcher foils below 10 MeV was avoided whenever possible.

The range of He^3 in the plastic foils was calculated from the element ranges of Williamson and Boujot according to Bragg's empirical formula[53]

$$\frac{1}{R_t} = \sum \frac{w_i}{r_i} ,$$

where

R_t = range of a particle in a given substance,
w_i = weight fraction of each element present,
r_i = range of the particle in the respective element.

The only ranges available for He^3 in carbon, hydrogen, oxygen, and fluorine are the calculated values of Demildt and of Williamson and Boujot. The results of these two computations are in fair agreement (about 4% for the plastics used at He^3 energy of 30 MeV, 2.5% at 15 MeV, and 1.5% at 7 MeV). An experimental range was determined for polystyrene, one of the plastics used, to verify these theoretical values. The results, which favor the longer ranges of Williamson and Boujot, are described in the next section under the specific procedures for the He^3 + C^{12} excitation functions.

4. Irradiation

The length of the bombardments varied between 10 and 25 minutes, according to product nuclide being studied. The average beam currents were about 0.010 to 0.100 μA of $He^3(++)$. These irradiation conditions produced suitable amounts of the product nuclide for convenient detection.

The total charge obtained from the bombardment was measured by a Faraday cup and an integrating electrometer. This electrometer was calibrated by passing a known current into it for a measured time just prior to each bombardment. The current source was a thermally insulated 1.019-volt standard cell and either a 100.0 or 1000.0 megaohm precision resistor. The conditions of intensity and scaling were the same as during the actual bombardment.

5. Counting Techniques

The positron emission rate of all samples was counted by means of end-window, gas-flow proportional counters. The detectors were standard aluminum cylinders of 1-inch inside-diameter with a window cover of 1/4-mil goldized Mylar. The collecting electrode, of 1-mil tungsten wire, was shaped in a 5 mm-radius semi-circular loop and supported in a hypodermic needle type fork. Methane gas was used in the counters which had backgrounds of 8 to 15 cpm. The stability and plateaus were checked with a Cl^{36} standard source which counted at 59,000 to 65,000 cpm on

Shelf 3 on the various counters used. Observed counting rates were normalized to a 63,300 cpm standard from the counting rate of the standard determined periodically during each experiment for each counter. The over-all detection coefficient, ODC, for each shelf and counter was also normalized to the 63,300 cpm standard. The resolving time of each of the counters was determined by the paired-source technique. These values ranged from 30 to 5.6 μsec. Corrections to high counting rates were applied when necessary. (See Appendix C.) Since the maximum positron energies of F^{18}, C^{11} and N^{13} vary from 0.65 MeV to 1.19 MeV,[54] the ODC was separately determined or estimated for each excitation function. The specific methods are given in the second part of this section where the reactions are considered individually.

The sample foils were mounted on 1/16-in. aluminum cards with double-faced Scotch tape and covered with 0.9 mg/cm^2 of Videne, a clear plastic foil (Goodyear Tire and Rubber Co.). They were counted at reproducible geometries in a conventional shelf assembly.

B. Experimental Procedures for Specific Excitation Functions

1. Production of F^{18} from He^3 Reactions with O^{16}

The material used as the oxygen source to determine this excitation function was Mylar, a condensate of terphthalic acid and ethylene glycol, which contains 62.7% carbon, 33.2% oxygen, and 4.1% hydrogen. The material was obtained from Hastings and Co., Philadelphia, Penn. Circles of 0.750-inch diameter were cut from 1/4-mil (0.93 mg/cm^2) Mylar sheets.

The variation in superficial density of the foils used was found to be about 1%. When single Mylar foils were used the recoils were caught in oxygen-free polystyrene foils which are described in the next section.

The over-all detection coefficient in the mounted samples was determined as follows: The positron counting rate of a sample of F^{18}

produced by the reaction of O^{16} with He^3 in 1/4-mil Mylar was determined with a 4π-proportional counter. The foil used was covered on both sides with a thin layer of aluminum (approximately 40 μg/cm^2) to make it conducting. Activities induced in the aluminum were insignificant. The correction to the counting rate for self-absorption of F^{18} positrons in the Mylar was determined by successively imposing aluminized Mylar foils on both sides of the activated one, recording the counting rate adjusted for decay at each absorber thickness, and extrapolating to zero thickness. The correction was found to be 1.7%. From the findings of Pate and Yaffe[55] a linear extrapolation is justified for a β-emitter of this maximum energy, 0.65 MeV. A correction obtained in a similar manner by these same workers for negatrons in VYNS, a polyvinylchloride-acetate copolymer, was approximately 2% at comparable thickness.

The absolute disintegration rate was then obtained by dividing the observed 4π-counting rate of the foil by 0.983 to correct for self absorption and by 0.97, the positron branching ratio,[54] the assumption being made that none of the soft x-rays or weak Auger electrons from the 3% EC branch are detected by the 4π-counter. This same source with the additional absorbers removed was then mounted in standard fashion and counted on various shelves of the end-window proportional counters. The observed counting rate (corrected for decay) at the proportional counter divided by the absolute disintegration rate is ODC. It was, for example, 0.123, on Shelf 4 (about 0.6 inch from the 1-inch diameter window). A complete listing of these coefficients is given in Appendix C.

The carbon and hydrogen in the Mylar do not interfere with the F^{18} detection; 4 hours after bombardment, when counting was begun, the 109.7-min F^{18} was the only nuclide detected, the 20.4 min C^{11} formed by the $C^{12}(He^3,\alpha)C^{11}$ reaction and the 10.0-min N^{13} from the $C^{12}(He^3,np \text{ or } d)N^{13}$ reactions having decayed to a very low level.

2. Production of C^{11} and N^{13} from He^3 Reactions with C^{12}

The plastic used as the carbon source was polystyrene (Trycite, Dow Chemical Corp.) which contains 92.3% carbon and 7.7% hydrogen. Circles of 0.812-inch diameter and 3/4-mil (2mg/cm^2) thickness were used. The variation in superficial density of the foils was as high as 10%. However, the polystyrene was supplied in a roll, some portions of which were uniformly thinner than others. Thus by weighing and judicious selection, foils of fairly uniform thickness were obtained. Polystyrene was chosen because it was available in thin films and more durable than the very similar hydrocarbon plastic, polyethylene. When the recoils were also counted, 0.1 mil gold foils were used as catchers.

The range of He^3 ions in polystyrene was approximately measured by bombarding a stack of accurately weighed, 3/4-mil polystyrene foils and determining the maximum penetration of reaction-producing beam by counting C^{11} from the $C^{12}(He^3,\alpha)C^{11}$ reaction. The deepest foil in which appreciable activity occurred was equivalent to a beam traversal of 92.5 to 94.8 mg/cm^2 of polystyrene. The energy of the He^3 ions at entry into the first polystyrene foil was 30.7 MeV; C^{11} production ceases at 3.8 MeV. At this energy Williamson and Boujot,[50] and Demildt,[49] give as a range for He^3 in polystyrene 2.6 mg/cm^2. Thus the total range for 30.7 MeV He^3 particles in polystyrene is between 95.1 and 97.4 mg/cm^2. The range of 30.7 MeV He^3 particles in polystyrene calculated from Williamson and Boujot is 96.7 mg/cm^2 and from Demildt 94.0 mg/cm^2. Consequently the former range-energy tables were used to compute the He^3 ranges in all plastic foils.

The ODC for C^{11} was determined in a manner analogous to that used for F^{18} in Mylar. About 35 μg/cm^2 of gold was deposited on 3/4-mil polystyrene foils by vacuum evaporation (gold was used here because of its being more tractable in the evaporator). One of the foils was bombarded in the He^3 beam below the Coulomb barrier for gold. The remainder were used as absorbers in the 4π-counting which was delayed until the N^{13} activity had reached a very low level. Self-absorption of C^{11} in the polystyrene foil was found to be 1.9%. The electron-capture branching of this nuclide is 0.19%,[54] thus the disintegration rate for C^{11} in this experiment was obtained by dividing the 4π counting rate simply by 0.979. Then on Shelf 4 of the end-window counter, the ODC was 0.136 (See Appendix C.).

It was not possible to determine experimentally the ODC for N^{13} in the polystyrene foils. Since the maximum $\beta+$ energy of N^{13}(1.19 MeV) is close to that of C^{11}, the ODC was assumed to be the same for both nuclides. Since the 10-minute N^{13} and the 20-minute C^{11} activities induced in the polystyrene foils were counted simultaneously, two-component decay curves resulted. These were resolved by means of a 7090 computer program (LENIC), which determines the activity at the end of bombardment, A_o, and the standard deviation of this value for each component.

3. Production of F^{18} from He^3 Reactions with F^{19}

The source of fluorine was polytetrafluoroethylene film (Teflon-Dielectrix Co., Queens Village, N. Y.), which contains 24.0% carbon and 76.0% fluorine. The plastic foils were 1/2-mil (2.7 mg/cm^2) thick and 0.812-in. diameter. The variation in thickness of these foils was about 1%. The three-foil recoil technique was employed in all the experiments. Polystyrene was used as the catcher foils.

The ODC for F^{18} in this matrix was estimated from the self-absorption and effeciency determinations described above for F^{18} in Mylar.

The Teflon foils were counted about four hours after bombardment to eliminate the C^{11} and N^{13} activity. The counting rate data conformed to a simple 109.7-minute half-life and was free from extraneous activity to level of less than 10 cpm from an initial total counting rate of about 10^4 cpm of F^{18}.

4. Production of N^{13} from He^3 Reactions with N^{14}

An attempt was made to determine the excitation function for the production of N^{13} from the He^3 bombardment of N^{14}. The nitrogen source was melamine-formaldehyde resin which contains 60.8% nitrogen, 34.8% carbon, and 4.4% hydrogen. Because the resin is not available in thin foils it was coated on 0.00025-inch gold foils. Counting techniques similar to those described above were employed. Due to the presence of oxygen impurities from residual formaldehyde and the large amount of carbon in the resin, too many interfering reactions occurred and inconsistent results were obtained above 7 MeV. Below this energy the thickness of the foils severely limited the number of target foils that could be irradiated. Between 4 and 6 MeV, the average cross section for N^{13} production appears to be approximately 20 mb. To obtain an accurate excitation function for this reaction it will be necessary to use an oxygen and carbon free target. The use of a nitride, such as tantalum nitride, is suggested.

C. Results and Discussion of Specific Excitation Functions and Mechanisms

The cross sections for the following excitation functions were calculated from Eqs. (1) and (2) in the first section. The energy of the He^3 beam at the appropriate foil position in the stack was determined from the range-energy relations discussed above. The horizontal bars on the points represent the energy loss of the beam in the foil. Vertical error bars are only approximate due to the difficulty in determining this uncertainty accurately. An estimation of the error in the cross section measurements is included in Section E. Because a correlation exists between the shape of an excitation function and the general reaction mechanism, we include in this section with our results the mechanism studies of other experimenters.

1. Excitation Function for Production of F^{18} from He^3 Reactions with O^{16}

The excitation function is shown in Fig. 3. This excitation function represents the sum of two reactions essentially: $O^{16}(He^3,p)F^{18}$ and $O^{16}(He^3,n)Ne^{18}$. The relatively high over-all cross section and in particular the 400 mb value at 7.5 MeV is the result of the enrichment of the direct F^{18} production by the β+ decay of Ne^{18} from the (He^3,n) reaction. The lowest He^3 energy at which these reactions may be induced is 4.5 MeV; the appreciable cross section 2 MeV below this value is attributed to the straggling associated with large beam-energy degradations (before target entry the beam already has a 2% energy spread) and perhaps to accumulated range-energy errors. The shape of the excitation function is not greatly changed by this except to lower the points plotted at the low He^3 energies and make the slope of the curve steeper in that region. Any fine structure is presumably smoothed out because of the target thickness, beam straggling and resolution, as well as because the cross section represents the sum of two reactions. A considerable number of angular distribution studies have been performed.[56-61] Middleton[60] considers the double stripping process to be the dominant mechanism at energies in excess of about 5 or 6 MeV for He^3 two-nucleon transfer reactions. Hinds and Hinds[60] indicate a direct process, two nucleon stripping, as the predominant mechanism for the $O^{16}(He^3,p)F^{18}$ reaction at an energy of 10 MeV. Gale, Garg, and Ramavataram[58] favor a direct interaction (double stripping as opposed to a knock-out mechanism) in the $O^{16}(He^3,n)Ne^{18}$ reaction as low as 6 MeV. The data of Towle and Macefield[57] suggests that a direct process is competing with compound nucleus formation at 6 MeV in the (He^3,n) reaction.

2. Excitation Function for Production of C^{11} from He^3 Reactions with C^{12}

The excitation function is shown in Fig. 4; at these energies it, almost exclusively, represents the $C^{12}(He^3,\alpha)C^{11}$ reaction. The broken

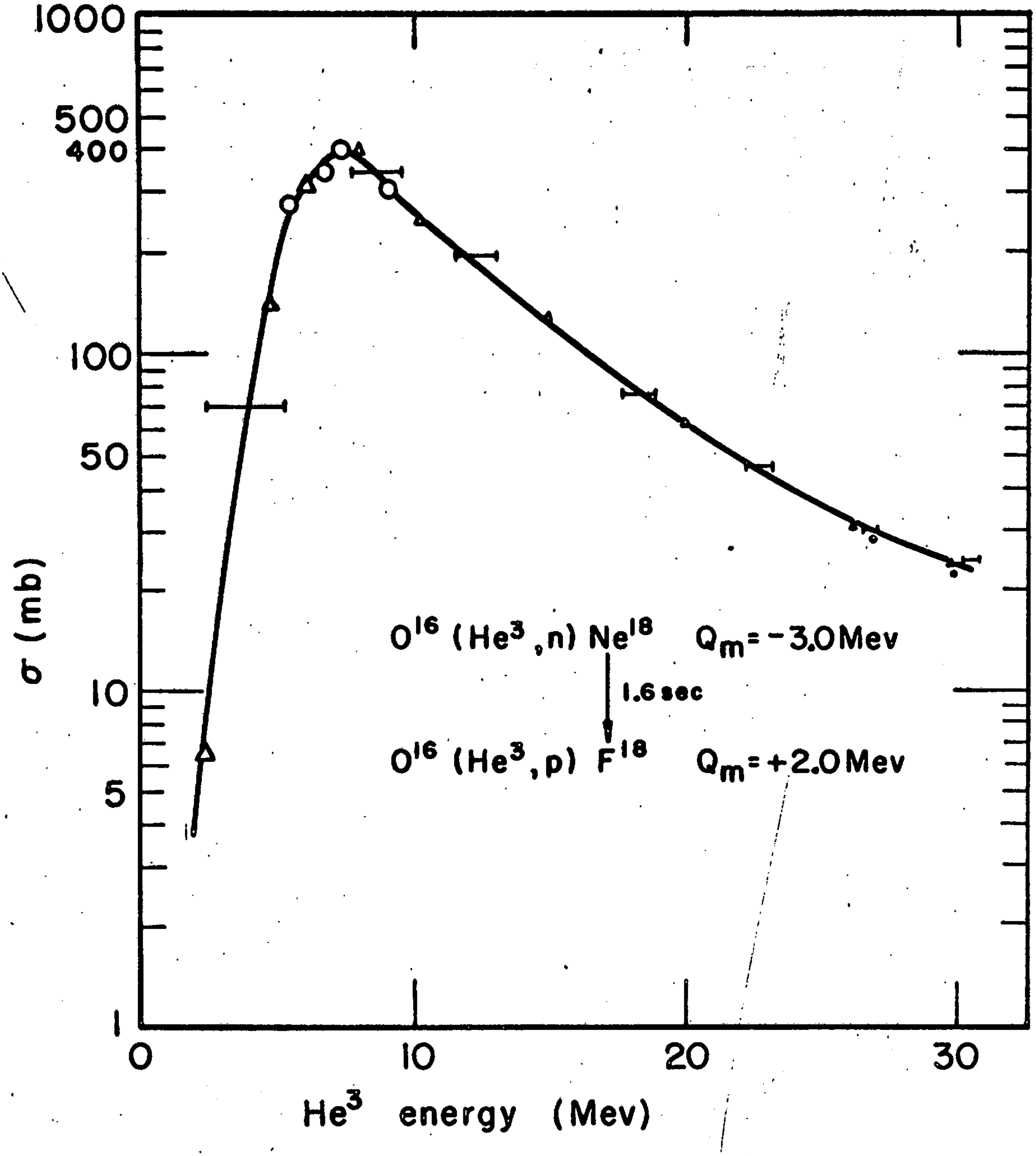

MU-24829

Fig. 3. Excitation function for production of F^{18} from O^{16} by (He^3, n) + (He^3, p) reactions.

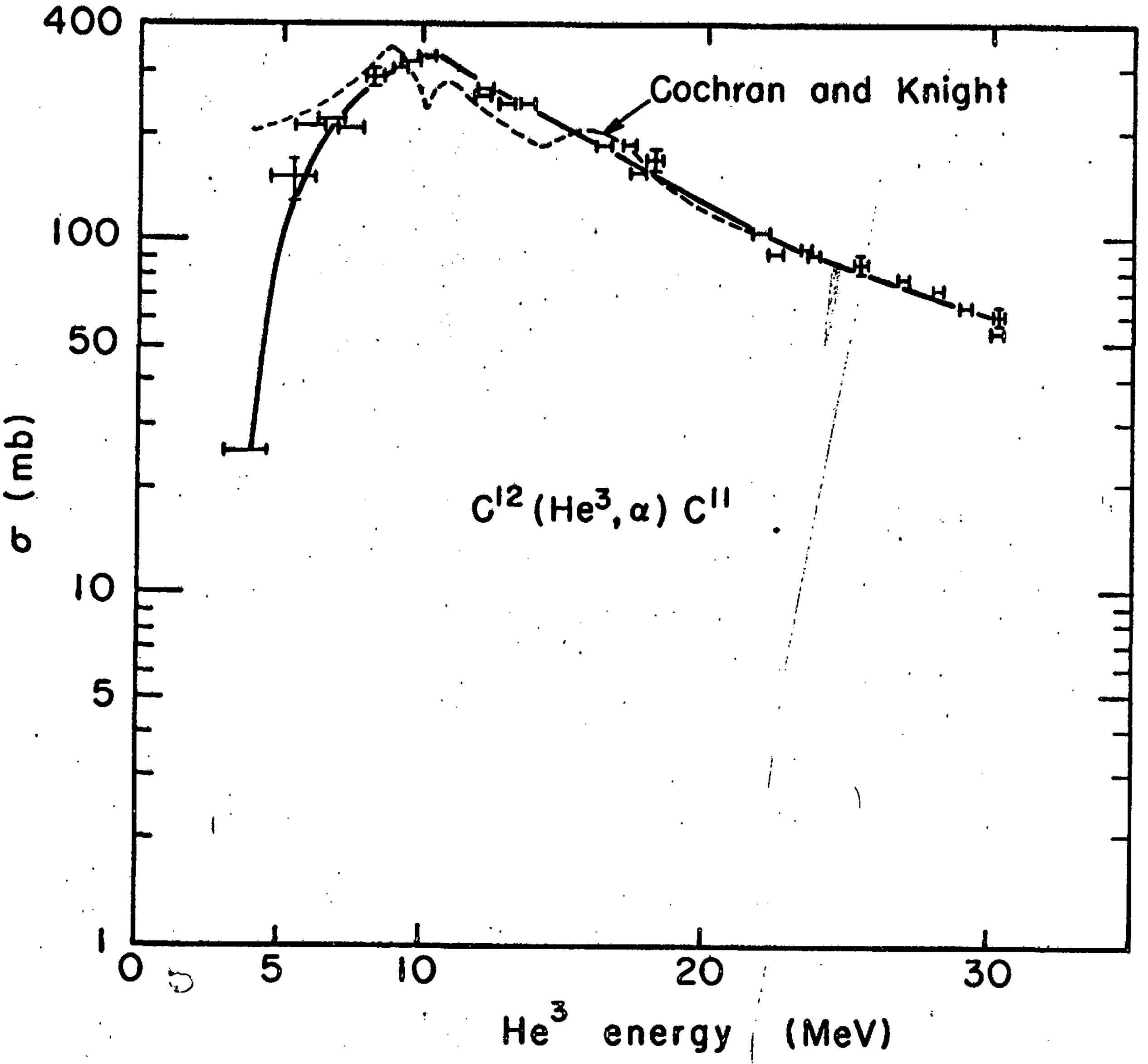

MUB-4612

Fig. 4. Excitation function for $C^{12}(He^3, \alpha)C^{11}$ reaction.

line indicates the results reported by Cochran and Knight.[62] They were able to obtain this fine structure, which is attributed to particle decay of excited states of C^{11}, because of their employing a variable-energy cyclotron with very well-defined energy resolution to accelerate the He^3 ions. Again the cross section obtained below 3.8 MeV is due to straggling and range-energy uncertainties.

The mechanisms by which this reaction proceeds are not fully elucidated. At very low energies (2.5 MeV) Bromley, Kuehner, and Almquist[63] have found that the analogous $O^{16}(He^3,\alpha)O^{15}$ reaction is strongly a compound-nucleus interaction. On the other hand at 2.0 and 4.5 MeV the $C^{13}(He^3,\alpha)C^{12}$ reaction favors some form of stripping mechanism.[64,65] Since C^{12}, like O^{16}, is a so called α-particle nucleus, we would expect a compound system to be the primary interaction mode for the $C^{12}(He^3,\alpha)C^{11}$ reaction at very low energies. At energies between 6 and 10 MeV Hinds and Middleton[66] have found this reaction to proceed predominantly by a direct process. Taylor et al.[67] have obtained similar results for the $O^{16}(He^3,\alpha)O^{15}$ reaction at 5.2 MeV. Pankratov and Serikov[68] report evidence for a direct process from 26 to 33 MeV for $C^{12}(He^3,\alpha)C^{11}$. However, the work of Aguilar et al.[69] and Garcia et al.[70] suggests that at 29 MeV while the formation of the 4.26-4.75 MeV (unresolved) doublet state of C^{11} is readily fitted by direct-interaction analysis, the ground state formation is not. At this same energy Sen Gupta et al.[71] have found that the (He^3,α) reaction for O^{16} leading to the 6.15 MeV excited state of O^{15} is not formed by a direct process alone. At 29 MeV, however, it is difficult to understand how any compound-system interaction can be present since the compound nucleus would have about 40 MeV of excitation energy associated with it. Simple α-particle emission does not seem a suitable decay channel at this excitation. The simultaneous and independent release of 2 neutrons and 2 protons is more conceivable.

3. Excitation Function for Production of N^{13} from He^3 Reactions with C^{12}

The excitation function is shown in Fig. 5. This excitation function, which was obtained simultaneously with that for the

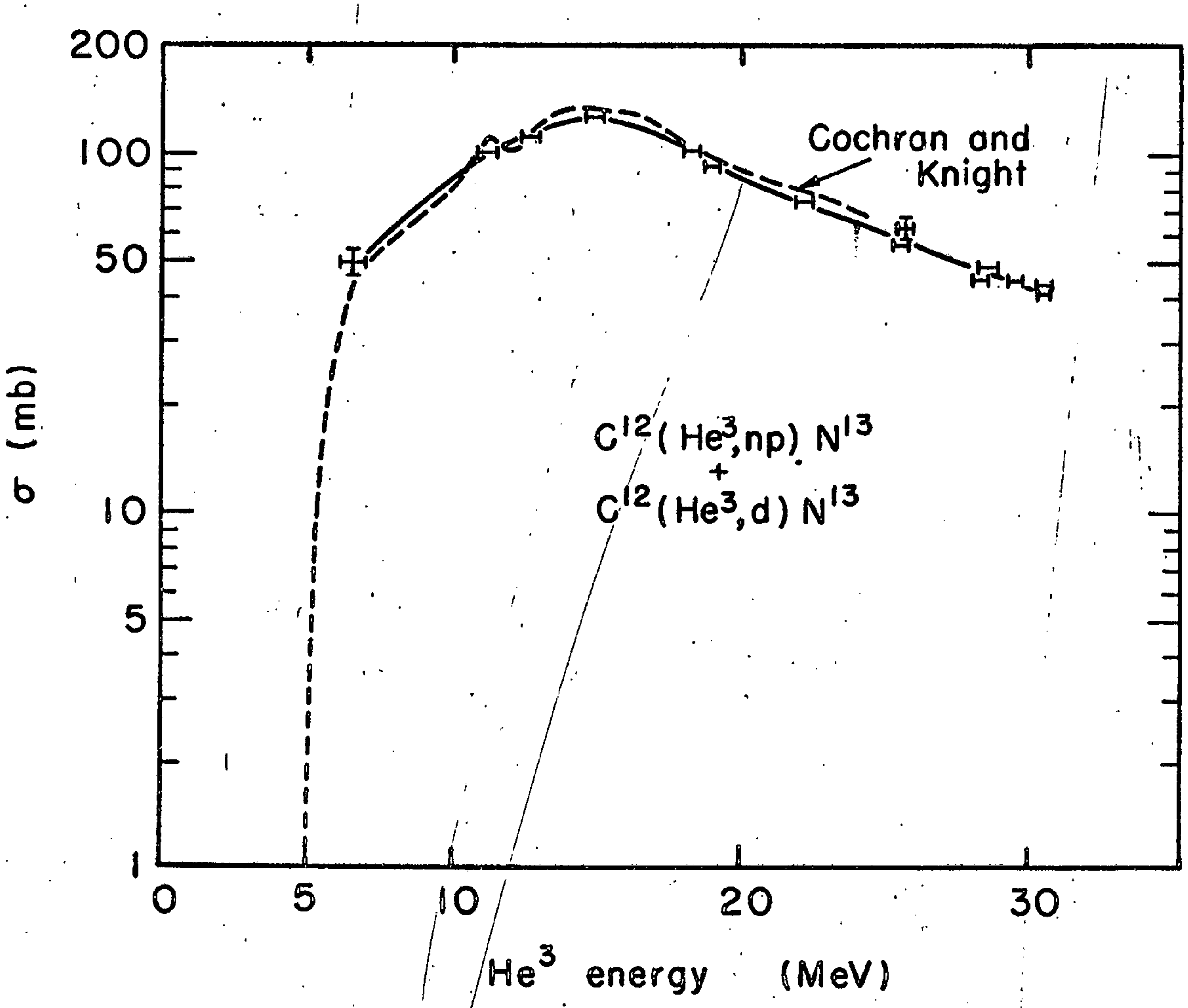

MUB-4615

Fig. 5. Excitation function for production of N^{13} from C^{12} by $(He^3, np) + (He^3, d)$ reactions.

$C^{12}(He^3,\alpha)C^{11}$ reaction primarily represents the $C^{12}(He^3,d)N^{13}$ + $C^{12}(He^3,np)N^{13}$ reactions. The 10-minute activity of N^{13} was resolved out of the 20-minute C^{11} activity by means of the LENIC computer program. The broken line represents the results obtained by Cochran and Knight[62] using a variable energy cyclotron. The rather low, maximum cross sections are to be attributed to the instability of all excited states of N^{13} to particle emission. The results reported here do not distinguish between the (He^3,d) and (He^3,np) reactions. By integrating the deuteron angular distribution data of Priest et al.[72] at 24 MeV Cochran and Knight[62] have found the contribution of the (He^3,d) interaction mode to be about 43%, 27%, and 24% at 14, 21, and 24 MeV respectively. Both Priest et al.[72] and Wegner and Hall[73] have obtained deuteron angular distribution which give good agreement with simple stripping theory.

4. Excitation Function for Production of F^{18} from He^3 Reactions with F^{19}

The excitation function is shown in Fig. 6. The cross section, which is primarily of the $F^{19}(He^3,\alpha)F^{18}$ reaction, is extremely low compared with the $C^{12}(He^3,\alpha)C^{11}$ reaction throughout the energy range studied. It is difficult to explain the apparently forbidden character of this reaction at low energies. The high positive Q-value of 10.1 MeV suggests that the peak for the reaction probability occurs below the coulomb barrier for the interaction of He^3 and F^{19}. This may account in part for the rather low cross section, but other factors seem to be responsible for the peculiar shape of the excitation function.

D. Discussion of Excitation Functions and Activation Analysis

The maximum cross section of about 400 mb for the formation of F^{18} from O^{16} occurs at 7.5 MeV and the maximum cross section of 320 mb for the $C^{12}(He^3,\alpha)C^{11}$ reaction, at 10 MeV. These high reaction probabilities at relatively low He^3 energies are favorable to activation

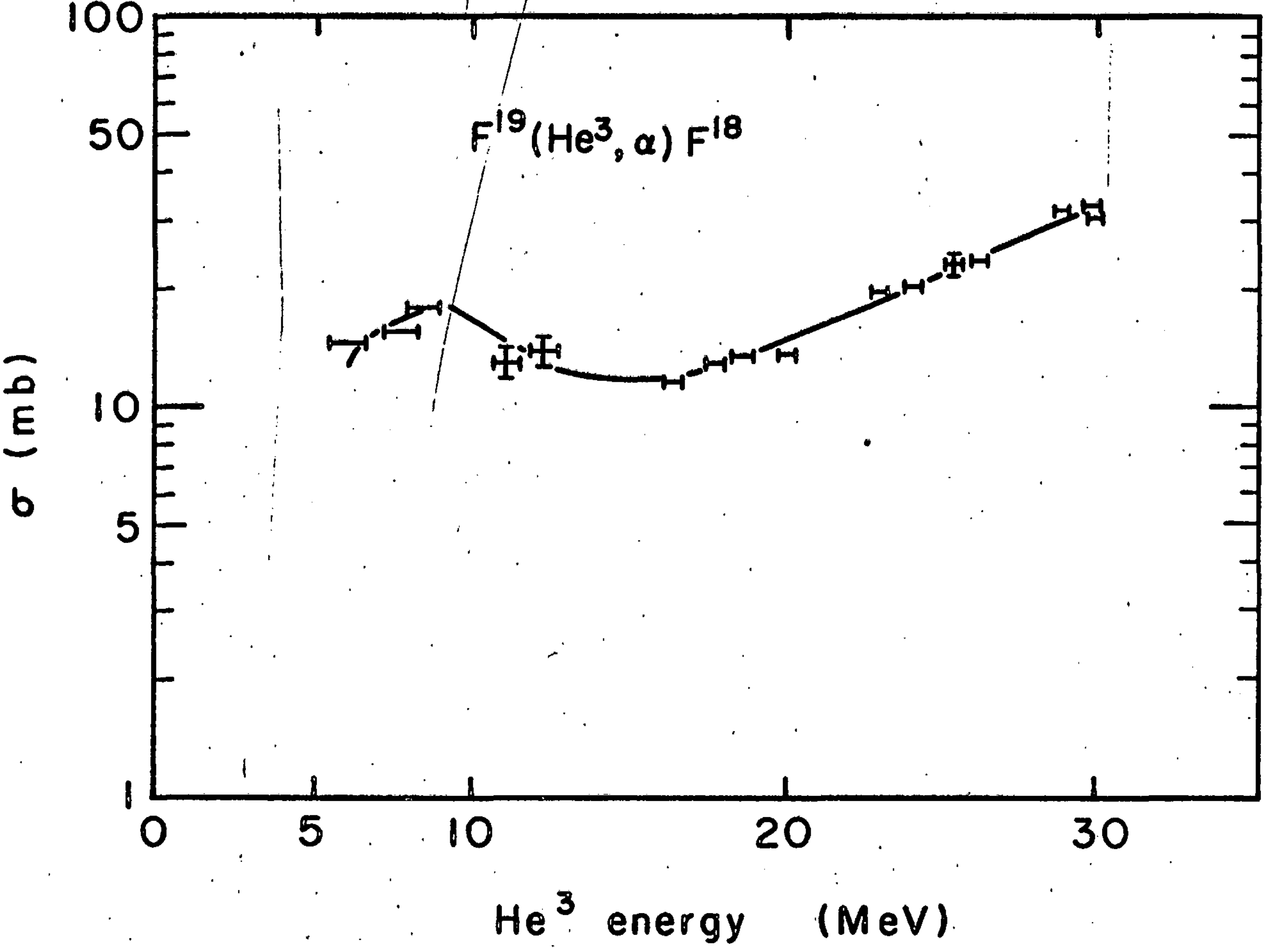

MUB-4614

Fig. 6. Excitation function for $F^{19}(He^3, \alpha)F^{18}$ reaction.

analysis of high sensitivity. The production of N^{13} from C^{12} will not interfere with either carbon or oxygen determinations because of the half-life difference. In fact, N^{13} may be used as a check on the results if nitrogen is known to be absent from the sample. The presence of sodium or fluorine would constitute an interference to oxygen determination as would boron or beryllium to carbon. In most of these cases another reaction or determination would have to be used, for example, fluorine in the oxygen sample by the $F^{19}(He^3,n)Na^{21}$ reaction; carbon in the presence of beryllium by the $C^{12}(He^3,n)O^{14}$ reaction (Na^{21} can not be produced from He^3 and O^{16}, nor O^{14} from He^3 and C^{12}).

At He^3 energies between 3.8 and 6 MeV the relatively high cross section for the $C^{12}(He^3,\alpha)C^{11}$ and $O^{16}(He^3,p)F^{18} + O^{16}(He^3,n)Ne^{18} \xrightarrow[1.5\ \text{sec}]{\beta+} F^{18}$ reactions compared to the negligible cross section for the formation of N^{13} from C^{12} implies that O^{16}, N^{14}, and C^{12} can be studies simultaneously in the same sample. The reactions, $O^{16}(He^3,\alpha d)N^{13}$, $O^{16}(He^3,2\alpha)C^{11}$, and $N^{14}(He^3,\alpha d)C^{11}$ have thresholds above 7 MeV. Nitrogen would be determined by the $N^{14}(He^3,\alpha)N^{13}$ reaction.

For the purpose of activation analysis the low reaction probability for F^{19} and He^3 represents a loss in sensitivity. However, from the point of view of interference in the determination of oxygen in the presence of fluorine, this difference of a factor of 10 to 20 at energies below 10 MeV between the cross section for the formation of F^{18} from O^{16} and from F^{19} is an advantage.

E. Discussion of Errors

In this section we present an estimate of the uncertainty of our results based upon the errors involved in determining each of the relevant parameters; an estimate of error based on replicates is not sensitive to systematic errors.

The uncertainty in the determination of the total charge received by the target is minimal. The integrating electrometer was calibrated before each bombardment by means of a standard cell and precision resistors that supply a current measured to an accuracy of better than 0.1%. Collimation was such to insure total reception of the beam by the target. Chronometry is reliable to at least 1%.

The half-lives of all the nuclides studied are known to an accuracy considerably better than 1%. The determination of the disintegration rate involves errors which including decay-curve analysis, cumulatively amount to about 2%. In this we include counter instability as well as counting statistics generally. The weighing of the foils introduces an error which is quite small in the case of Mylar and Teflon because of their 1% uniformity of thickness. However, the superficial density of the polystyrene foils must be assigned an uncertainty of 5%. The problem of recoil gas loss had to be considered. This loss is a hot-atom diffusive loss not related to the previously considered fast-recoil loss from the reaction itself. It is possible that C^{11}, N^{13}, and F^{18} can escape into the Hilac vacuum during irradiation, or after irradiation when the stack is separated and mounted. After mounting no further gas loss can occur because the foil is covered and sealed on the aluminum card. (The fact that the observed half-life of C^{11} always corresponded with the published value supports this conclusion.) The probability for diffusive gas loss is much higher during irradiation because of the heat generated in the target by attenuation of the beam. Cochran and Knight[62] have observed that open and sealed targets of Teflon 1/2-mil (approx. 2.5 mg/cm^2) and polyethylene (approx. 1.5 mg/cm^2) gave results that fall within the 5% scatter inherent in their measurements. And thus they concluded that in their open stacked-foil bombardments no more than 5% of the C^{11} and N^{13} escape as gaseous oxides or hydrocarbons. Cummings et al,[74] however, have reported up to 15% loss in proton bombardments of approx. 5 mg/cm^2 polyethylene foils, and up to 7% loss in approx. 2 mg/cm^2 polystyrene foils.

In our work the close (5%) agreement for mylar and polyethylene, for oxygen and/or carbon. Section V,4, and Teflon for carbon and fluorine, Section V,5, to give the empirical formulas with the use of open stacked-foils indicates that the diffusive gas-loss of C^{11} and F^{18} was less than

5%. This conclusion is supported by the fact that when thicker foils were used the same results were obtained. In Teflon, perhaps, the diffusive recoil loss of C^{11} is prevented by the lack of hydrogen to make volatile species; in metals, by carbide formation.

Multiple experiments were performed to determine each excitation function. In the case of $C^{12}(He^{3},\alpha)C^{11}$ and $C^{12}(He^{3},np \text{ or } d)N^{13}$, with target foils of less reliable thickness, ten experiments were carried out; for the $O^{16}(He^{3},p)F^{18} + O^{16}(He^{3},n)Ne^{18} \xrightarrow[1.5\ \text{sec}]{\beta+} F^{18}$ reactions, six, and for the $F^{19}(He^{3},\alpha)F^{18}$, three. Thus notwithstanding the additive property of the uncertainties considered above, the smooth-curve cross sections reported represent averages and consequently are more reliable than the sum of the various errors. An over-all standard deviation in the cross sections of about 5% would not seem excessively optimistic.

V. ACTIVATION ANALYSIS: EXPERIMENTAL PROCEDURES AND RESULTS

In the following sections we describe the absolute and the relative method of analysis by He^3 activation which have been used at this laboratory as a consequence of the reaction studies reported herein as well as certain specific analyses.

A. Absolute Method

The first method, absolute analysis, employs the thin-target procedure. It is simply an extension of the stacked-foil technique used to determine excitation functions. A thin foil of the material to be subjected to analysis is placed between suitable catcher foils in a stack of degraders. The catcher foils must be of material that will not contaminate the sample from extraneous sources of the radioactive nuclide being studied. The sample is placed in the stack at an energy determined from consideration for both maximum cross section and the elimination or minimization of interfering reactions. At times it is not possible to utilize the maximum cross section, however, because of limitations imposed by the thin-target approximation or cross-section integration over the beam-energy decrement in the foil. Surface etching or grinding may be necessary for analysis of samples that react with or absorb any of the atmospheric gases. The same counting and irradiation procedures may be used in the analysis as in the determination of excitation functions. The determinations in which this method was used are described below.

1. Analysis of Thorium for Oxygen

In order to determine the utility of this method to detect a light nuclide in a host material which is itself radioactive, S. B. Hingorani and the author attempted to analyze thorium for O^{16}. Foils of 35 mg/cm^2 thickness were mechanically cleaned and washed in a nitrogen atmosphere. Each was then sealed in a 2.0 mg/cm^2 polystyrene envelope because of the reactivity of thorium with oxygen and irradiated for about 14 min with a beam intensity of 0.010 μA at energies of 11.1 and 17.1 MeV. Determination of 109.7-minute F^{18} was accomplished by ordinary positron counting and by a 3 × 3 inch NaI(Tl) scintillation counter and 100-channel pulse-height analyzer which were calibrated for annihilation radiation. The samples, in which annihilation radiation was counted, were placed between 50 mil copper plates. A pulse height spectrum is displayed in Fig. 7. The 0.511-MeV full-energy peak from F^{18} positron annihilation in the source was greater in intensity than the γ-ray background from the thorium daughters by a factor of about 30 in the annihilation energy channels. The sample shown had decayed through 2.4 F^{18} half-lives (268 minutes after bombardment). The decay of the full energy peak, which confirms that the positrons are from F^{18}, is given in Fig. 8. The signal-to-background ratio could have been enhanced by factor of 100 or more by increases in beam intensity and bombardment time.

The results of this absolute analysis gave 0.61 ± 0.06% O^{16} by weight. The thorium samples were analyzed at the Lawrence Radiation Laboratory, Livermore, by the vacuum fusion technique. Thorium was fused in a graphite crucible, and CO and CO_2 were measured. The results obtained thereby gave 0.35% oxygen by weight. Although these differ from each other by more than the experimental uncertainties, later results, referred to below, and in the following section give better correlation between the two methods.

2. Analysis of Gold for Carbon and Oxygen

Thin gold foils of 0.0001-in. thickness (8.4 mg/cm^2) and 1-in. diameter were washed with distilled water and acetone and irradiated in a stacked-foil target for approximately 15 minutes at 0.01 μA. The gold foils were placed at about 10-MeV He^3 energy in groups of three; only the center foil was counted. Positrons corresponding to 20.4-minute C^{11} and 109.7-minute F^{18} were counted in standard end-window proportional counters where the ODC for each nuclide was known. The decay curves, which included 10.0-minute N^{13}, were analyzed by the LENIC program. The results of this absolute analysis were 0.006% O^{16} and 0.01% C^{12}. Ryan, Green and Lowenhaupt[75] report a comparable level of oxygen in pure gold by He^3 irradiation in a rotating target. In their relative analysis a SiO_2 standard and coincidence counting of the 0.511-MeV annihilation radiation were used.

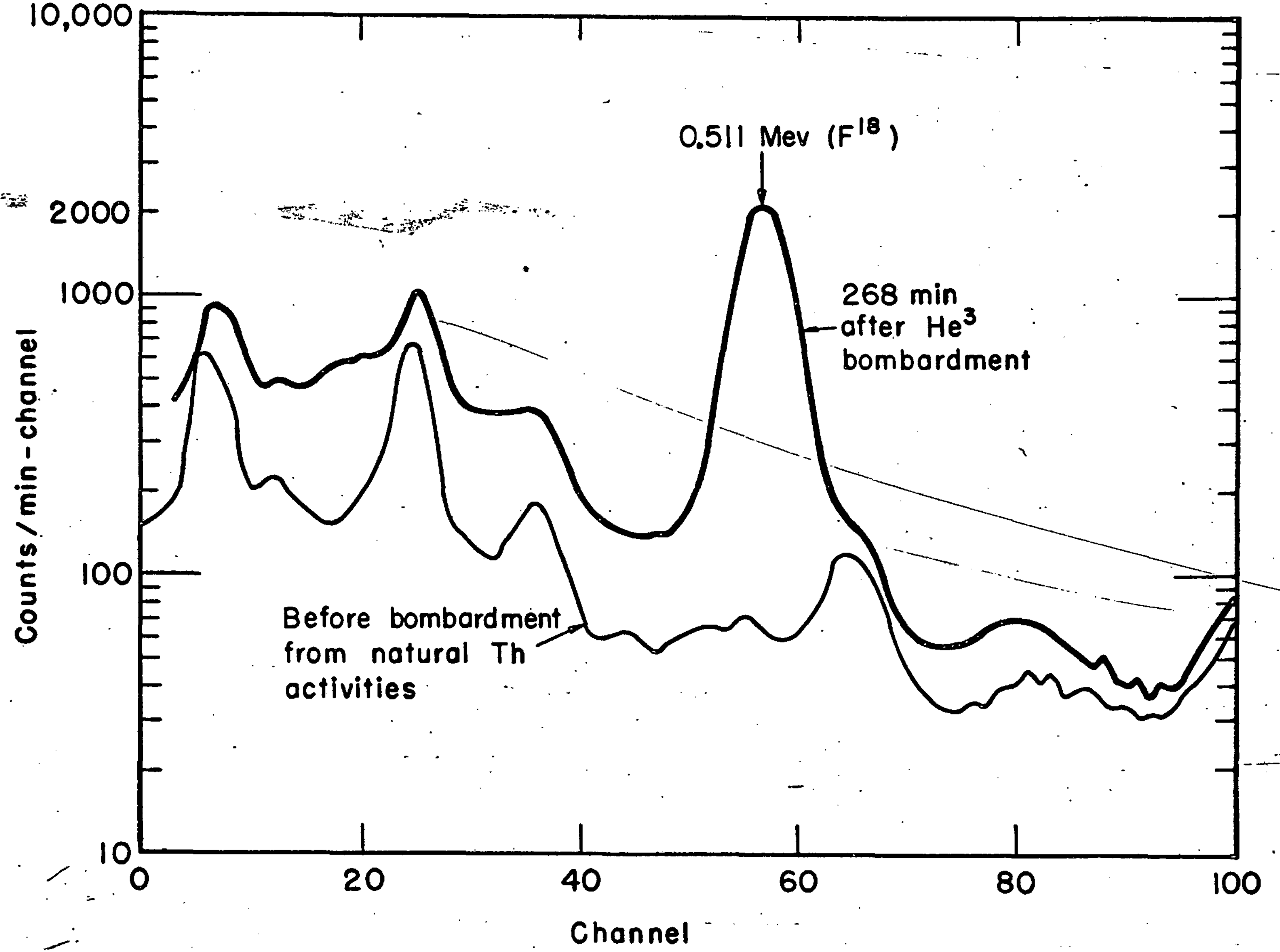

MU-24831

Fig. 7. Gamma-ray spectrum from thorium foil before and after He^3 activation.

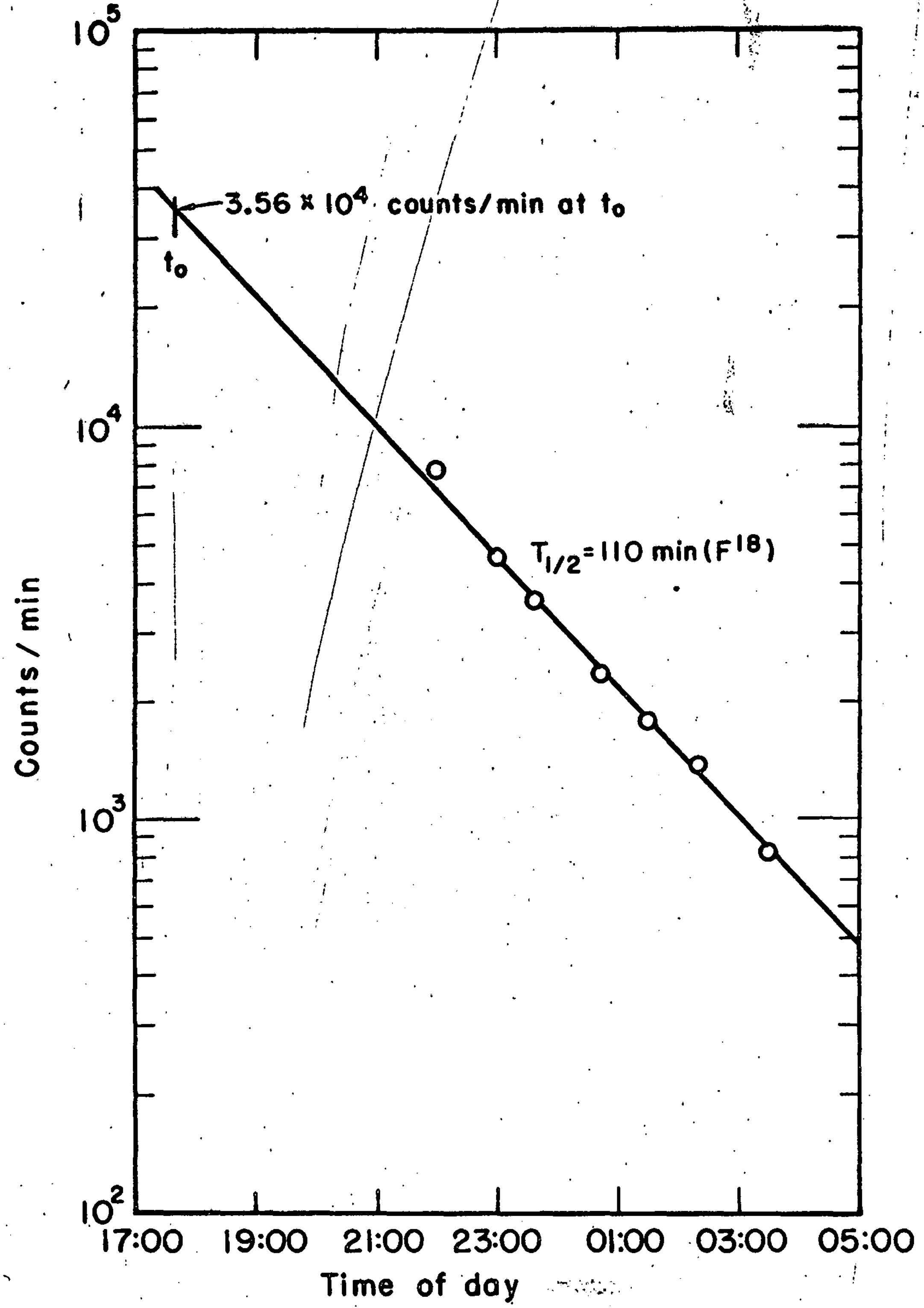

MU-24830

Fig. 8. Decay of full-energy peak (0.51 MeV) in thorium analysis.

3. Analysis of Silicon for Carbon and Oxygen

Silicon wafers measuring 1 inch in diameter and weighing approximately 30 mg/cm^2 were irradiated with 18- and 6-MeV He^3 ions in a stacked-foil target. The average current was 0.01 μA; the bombardment length, 15 minutes. In a second irradiation the beam intensity was increased to 0.02 μA; the duration was again 15 minutes. The resulting activities in some of the foils were measured by end-window β-proportional counting, in others by a 3 × 3-in. NaI(Tl) scintillation counter and 400 channel analyzer which were calibrated for annihilation radiation. A representative 0.511-MeV photopeak decay is shown in Fig. 9. The β-decay curves, which contained both 20.4 MeV C^{11} from C^{12} and 109.7 MeV F^{18} from O^{16}, were analyzed by the LENIC program. The results from the various foils and counting techniques averaged 0.13 ± 0.02% O^{16} and 0.24 ± 0.03% C^{12}.

These contents are undoubtedly quite high in part due to a thin layer of oxygen which is always present on the surface of elementary silicon. In our experiments, the silicon was washed with distilled water and acetone before bombardment; the wafers were too brittle to be mechanically cleaned by grinding. Chemical etching was not feasible because measurement of the amount of silicon removed was not possible. However, 0.13% oxygen and even higher, 0.24% carbon cannot be explained by surface contamination alone.

The exact process by which the silicon used for these wafers was made is not known. However, oxygen and carbon can easily be present as impurities in silicon. If the silicon is prepared in a quartz crucible, $SiO_{(g)}$, which has a vapor pressure of about 10 mm Hg at 1412°C, the melting point of silicon, can vaporize at an appreciable rate according to the equation

$$Si_{(\ell)} + SiO_{2(s)} = 2SiO_{(g)}$$

and thus become incorporated into the silicon piece. Carbon is also a common crucible for molten silicon, thus it is possible that some carbon dissolves since carbon and silicon are chemically similar.

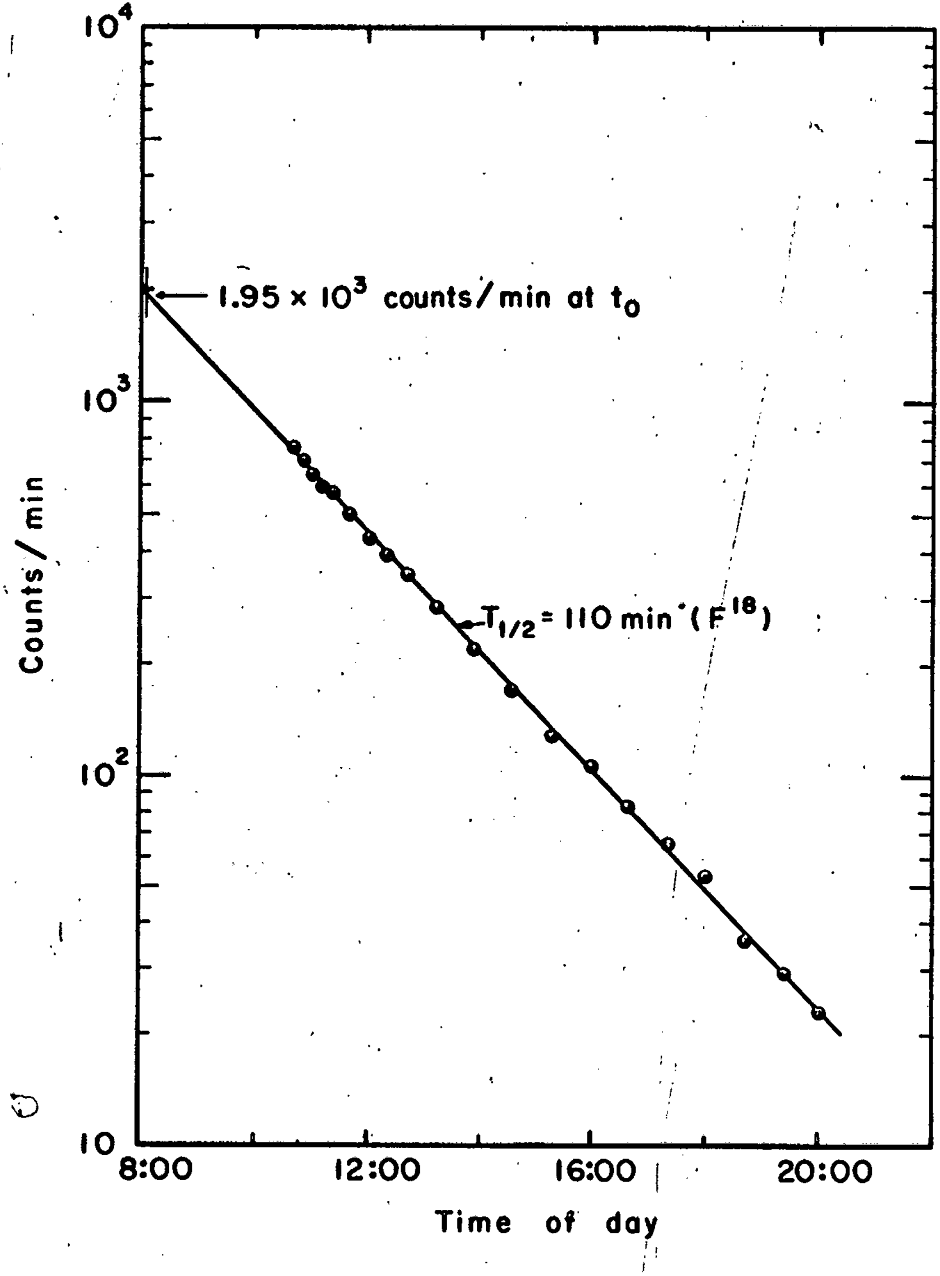

MUB-4616

Fig. 9. Decay of full-energy peak (0.51 MeV) in silicon analysis.

When silicon is melted by the floating zone process, no crucible is used; however, oxygen may still be present for Kaiser, Keck, and Lange[76] have shown that oxygen will readily dissolve in the silicon melt and become incorporated into the crystal. According to Tanenbaum,[77] boron is a common impurity in fused silicon, thus part of the C^{11} may be formed from $B^{10}(He^3,d \text{ or } np)C^{11}$, instead of $C^{12}(He^3,\alpha)C^{11}$.

Saito, Nozaki, and co-workers[78] have analyzed silicon by alpha-particle irradiation and subsequent grinding of the sample. In the first 2 mg/cm^2 they report about 80 ppm oxygen; below a depth of 5 mg/cm^2 they have found that the bulk oxygen content varied from 0.1 to several ppm in various types of silicon. They suggest that this method can be applied to the determination of carbon also.

4. Analysis of Mylar and Polyethylene for Carbon and Oxygen

These plastics (1/4 mil Mylar and 1 mil polyethylene foils) were treated as unknowns and subjected to carbon and oxygen analysis by conventional stacked-foil irradiations. Mylar gave results of 33% oxygen and 63% carbon which agree with the known composition of this material. Polyethylene gave a result of 86% carbon and about 0.01% oxygen impurity; the carbon content corresponds to the known composition of polyethylene, the oxygen level, which varied considerably among the samples, is probably due to surface contamination and occlusion during the rolling of the sheets. The agreement, for these macro-samples, with the known empirical composition, is evidence that the beam intensities, cross sections, and overall detection coefficients, are accurately known; these are the major sources of error for the absolute method.

5. Analysis of Teflon for Carbon and Fluorine

Again using the stacked-foil technique and β end-window proportional counting, a Teflon foil was treated as an unknown in a He^3 irradiation. Carbon was determined from the $C^{12}(He^3,\alpha)C^{11}$ reaction and fluorine from the $F^{19}(He^3,\alpha)F^{18}$ reaction. The results, 24% carbon and 76% fluorine, were in accord with the known composition of this plastic, again indicating accurate knowledge of beam intensities, cross sections, and overall detection coefficients.

B. Relative Method

1. General

The results of Sec. 4 and 5 of the previous Part A indicate that it is possible to obtain accurate analyses by the absolute method for thin targets. (A "thin" target is one in which the intensity of the beam does not diminish as the beam traverses the target; variations of the energy of the beam as it traverses the target are taken into account through prior measurement of the excitation functions.) In analogy with activation analysis by neutrons, it is possible, however, and convenient, to employ a "relative" method of charged particle analysis wherein it is not necessary to know the values of the cross sections, beam intensities, irradiation times, and overall detection coefficients. What is necessary however, is that a "standard" of known composition be irradiated and counted under identical (or nearly identical) conditions as the sample of unknown composition. While it is easy to count the radiations, especially gamma rays, from both standard and unknown under identical conditions, it is a subtle and often difficult task—both for neutron and charged-particle irradiations—to assure that the irradiation conditions are actually identical.

For neutron irradiations in neutron reactors, sample and standard are often irradiated in vials side-by-side and the assumption is implicitly made that both receive the same neutron flux, the same both in intensity and energy distribution. However, in many reactors, and in a given reactor, the flux and energy distribution varies with distance from the fuel or core. Also, the meaningful flux is that received within the sample itself, not that which is at the given reactor position; because of sharp neutron resonances, self-absorption and self-shadowing in the samples, which are functions of gross sample composition, must be taken into account even in the relative method. Analogous concerns are evident in fast-neutron irradiations in which the small d-t accelerators are currently being used for analysis.

While important advantages of the He^3 activation analysis method are that sharp nuclear resonances, if any, are smoothed out by the experimental technique employed, and that the cross sections for similar reactions do not change greatly in magnitude from element to element, care must be taken in a relative method to assure irradiation under identical, or nearly identical conditions. The next paragraphs discuss various modifications of the charged-particle relative method.

2. Relative Method with Thin Sample and Thin Standard

It is possible in the same beam to irradiate in the same stacked-foil sandwich both the unknown and the standard, if both are thin with respect to the total range of the incident beam. Many thin samples can be analyzed in the same irradiation. This, of course, will depend on the total energy of the beam available, 31-MeV He^3 for the present work but possibly less if a small cyclotron is used. Figure 10a shows such an arrangement. The beam is collimated into the center of the stack. The appropriate range-energy relations and the excitation functions must be used to correct the yield for the loss in energy as the beam traverses the stack, if the variation in beam energy causes significant change in the production cross section. The production cross section is an average over the beam-energy entering and leaving the given foil. It is not actually necessary to know the variation of absolute cross section with energy; it suffices to know the relative variation for the production of a given nuclide with beam energy. If, however, the absolute cross section is known as well as the integrated beam current and ODC, this "relative" method can be used in the same irradiation as a check on the absolute calibrations. An example of this system is the analysis of oxygen in 7 mg/cm^2 aluminum, in the same stack in which, at a close position, a Mylar standard of known thickness is placed.

A simple variation of the above is the irradiation of the sample in one stack, followed by the standard in an identical stack, in two successive bombardments. This would eliminate the need to correct for the possible difference in cross section mentioned above because both sample and standard would receive the same energy beam. The intensity and length of each irradiation would be easily measured with any beam-monitoring system, relative or absolute, i.e., scintillation counter placed near the target or a calibrated Faraday cup. This system is illustrated in Fig. 10b.

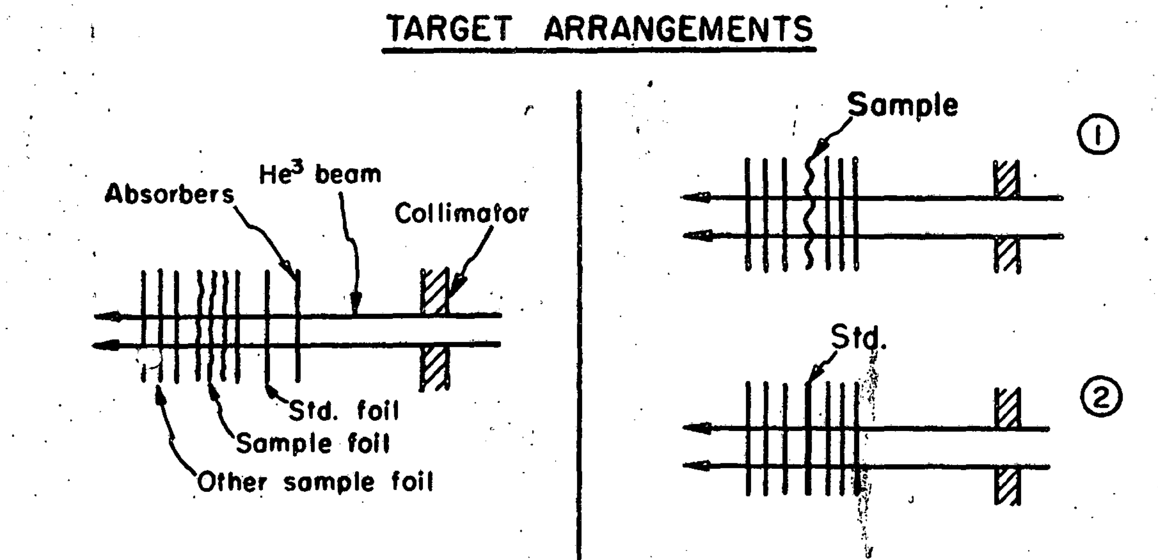

(a) Thin-sample, thin-standard, in same stack.

(b) Thin-sample, thin-standard, for two successive irradiations.

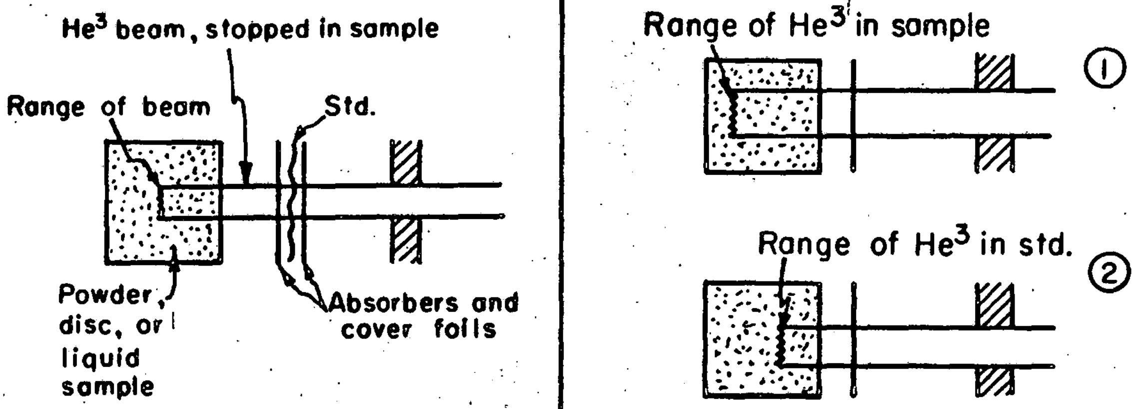

(c) Thick-sample, thin-standard, in same stack.

(d) Thick-sample, thick-standard, for two successive irradiations.

MUB-4664

Fig. 10. Various target arrangements for He^3 activation analyses by the relative method. (Schematic)

3. Relative Method with Thick Sample and Thin Standard

In many cases, samples may be in a form where it is difficult or inconvenient to prepare thin foil samples. Such might be powders, bulky pieces, or liquids. It is then useful (for solids) to prepare the sample in the form of a powder of thickness greater than the range of the incident He^3 beam. The powder is placed in a suitable holder, covered with appropriate absorbers and the thin foil standard, and the beam is collimated into the "stack". Both standard and sample thus receive essentially the same intensity beam up to the range of the beam, but the total production of the observed nuclide in the sample is obtained by graphical integration of the excitation function (absolute or relative) while the production cross section for the observed nuclide in the standard is taken from the excitation function (absolute or relative) directly. This system is illustrated in Fig. 10c.

4. Relative Method with Thick Sample and Thick Standard

In order to irradiate a thick powder and a thick standard, two successive irradiation must be carried out. An example of such a system would be the determination of oxygen in lead powder relative to the known oxygen content of a thick "foil" of quartz, SiO_2. It is necessary to correct for the different ranges of the He^3 beam in the sample and in the standard, i.e., lead and quartz in this particular example. It is necessary to monitor the integrated beam on each target. In the normal case, the area of the beam is less than the area of the sample and standard, because there is sufficient sample and standard available. This system is shown in Fig. 10d.

C. Results of Some Analyses

Because of the limit of available sample material, Demildt[79] modified our experimental procedure, for the determination of oxygen in actinide metals. He had at most about 1 mg of actinides and not in foil form. Basically this modification involved the use of the thick-sample, thin-standard method described above. The standard was an anodized 7 mg/cm^2-aluminum foil previously calibrated against quartz. The area of the target, however, was less than the area of the incident He^3 beam; the beam "bathed" the target which was 1/8-inch in diameter. Demildt's results for O^{16} in thorium averaged 0.52%; 0.6% was obtained by the vacuum-fusion technique. These values compare favorably with the result obtained by Hingorani and the author (0.61%) using the absolute-thin target method of analysis. The vacuum-fusion result (0.35%) reported on those samples was unexplainably low.

A further experimental modification, basically in the thick-sample, thick-standard method described above, was made by Demildt[80] and by Green.[81] The target area was again less than that of the He^3 beam. A rotating target assembly was adopted which permitted the irradiation of six platinum-encapsulated samples, including a quartz standard, by the beam in the same bombardment. Thus, the samples and the standard received the same intensity beam. However, because of the sample-holder design each position received somewhat less than 1/6 of the total integrated beam falling on the assembly. This rotating target assembly was also used by the author for several analyses for reasons of convenience, but in most analyses, it is not necessary to have such a small sample diameter (1/16 inch), which, aside from the disadvantage of small size, also necessitates a separate measurement of the area of both sample and standard.

Because of the high reactivity of thorium and other metals with atmospheric oxygen, weighing and scraping of the samples was done in a box with a nitrogen atmosphere. The samples were also vacuum-sealed and analyzed at Livermore for oxygen by vacuum-fusion method. The result of Ryan, Green, and Lowenhaupt[75] for O^{16} in thorium, 1060 ± 220 ppm, compares well with the result obtained by vacuum fusion on the same sample, 1160 ppm.

The difference in sample preparation prevents a real comparison of 1060 ± 220 ppm with Demildt's value of 0.6% (6000 ppm) or our value of 0.61%. In the same paper simultaneous analyses for O^{16} and C^{12} in terbium are reported; curium and americium were analyzed for O^{16} only.

Using the available rotating target assembly of Demildt[80] and Green,[81] G. Butler, M. Reed, and the author analyzed for oxygen, samples of niobium, lead, and beryllium. Thorium was included as a means of comparison with the work of Ryan et al;[75] quartz was used as the standard.

The Coulomb barriers for beryllium, niobium, lead, and thorium are 2.1, 13.2, 21.4, and 22.8 MeV, respectively. To prevent interferences from nuclear reactions of He^3 with the metal itself, an aluminum foil covering the targets was used to degrade the beam below 13 MeV.* For beryllium it was necessary to separate from the decay curve the 20.4-minute C^{11} activity produced by the $Be^9(He^3,n)C^{11}$ reaction. In the other metals only the 109.7-minute F^{18} activity was present.

The samples were small disks of quartz or metal which were 1/16 inch in diameter and about 1/64 inch thick. The niobium and thorium samples were very carefully scraped in a dry nitrogen atmosphere to remove any surface oxygen contamination. The lead, which was originally in powder form, was pressed into a disk of the above dimensions in the nitrogen dry-box. Within experimental error the disks thus obtained had the same density as natural lead. The relative areas of the samples were determined by means of a microscope and <u>Camera Lucida</u> without removal from the dry-box. Finally each disk was sealed in an evacuated platinum capsule by cold welding using a hydraulic press at 1200 psig.

---

*In one experiment, the aluminum cover was not thick enough to degrade the beam below the Coulomb barrier for the reaction of He^3 with niobium. The positron-annihilation decay curve obtained by coincidence counting was easily resolved into four components by FRENIC.[80] The half-lives of these components were 52 min, 110 min, 293 min, and 20 h corresponding to Tc^{94}, F^{18}, Tc^{94m}, and probably Tc^{95}. If this last assignment is correct then this Tc isotope, contrary to a previous report,[81] must decay by positron emission as well as electron capture. The β^+ activity was quite small, however. On the basis of these data above no estimate of the percentage of positron decay can be made.

The average beam current during irradiation was 0.15 to 0.30 μA of He^3 (++). The total charge received by rotating the target assembly was 1.0 to 1.60 μA. Each sample derived, however, less than one-sixth of the total. After bombardment the platinum capsule was opened with a scalpel and the sample was mounted without loss of material on a standard 1/16-inch thick aluminum card in a 1/4-inch diameter aluminum pod.

The positron-emission rate of the F^{18} produced in the samples at the end of bombardment was determined by measuring the decay of the 0.511-MeV full-energy annihilation peak. A coincidence counter consisting of two NaI(Tl) scintillation detectors in conjunction with a 100-channel pulse-height analyzer, calibrated with a Na^{22} standard for annihilation radiation, and a conventional scalar were used. The coincidence background was about 4 cpm in the area of the 0.511-MeV peak.

The ranges of the He^3 ions in the different metals and the quartz were obtained or calculated from Williamson and Boujot.[50]

The weight fraction of oxygen in the metals was calculated from Eq. (8). The results are tabulated in Table I.

This thorium result (860 ppm) compares favorably with those obtained by Ryan et al.[75] (1060 ± 220 ppm).

The beryllium samples were supplied by Nuclear Metals, Inc. The results obtained on them by the Texas Nuclear Corporation using fast-neutron activation analysis for oxygen by the $O^{16}(n,p)N^{16}$ reaction were

Beryllium, Distillate No. 15	81 ± 28 ppm
Beryllium, Vacuum-melted Pechiney Flake	302 ± 25 ppm

That our results for beryllium are possibly high is most probably due to surface contamination. The beryllium sample had to be chipped from the piece supplied and roughly shaped to the appropriate dimensions without scraping because of the hardness of the metal.

The niobium samples were taken from a rod which was supplied by the E. I. DuPont de Nemours and Company. Samples of this material have been analyzed for oxygen with the vacuum fusion technique by 18 different laboratories. The average value obtained was 49 ± 3 ppm. The reasons for our value, 101 ± 5 ppm, being higher are not known at this time; the

Table I. Oxygen contents in various samples analyzed by the thick-sample, thick-standard method.*

Metal		ppm oxygen
Thorium, Commercial		860
Beryllium, Distillate No. 15		120
Beryllium, Vacuum-melted Pechiney Flake		430
Niobium		106 100 96
	Average	101 $\sigma = 5$
Lead		1970 1690 1580 1460 1380 1180 1020
	Average	1470 $\sigma = 290$

---

*Rotating target used. Samples only 1/16 inch diameter.

extremely small sample size (6.7 mg) necessitated by the rotating target assembly may well account for part of the discrepancy.

The lead was received in powder form from Stanford University, Palo Alto, California. No other analysis was available on this material. The limitations of the rotating target assembly, which was used here because it was the only apparatus available for a thick target analysis, are reflected in the 20% precision of the results. The small sample size for a powder target unnecessarily compounds the errors in an analysis; rarely will the sample material be so limited that the beam must completely immerse it. With apparatus designed for ordinary sample handling we expect the precision would improve considerably.

D. Errors in Analyses

Ideally, the error in the absolute analyses should be in the same range as that in the determination of the production cross sections. In the case of the plastic materials such an estimation is probably justified. However, for the metal and silicon foils used an error of ±15% must be assigned primarily because of the statistical uncertainty of the low counting rates and sample handling techniques.

In the relative analyses the uncertainty is between 15 and 20% due to the restrictions of the available apparatus with respect to sample size, preparation, and handling.

VI. SUMMARY

The He^3 activation analysis method offers a new analytical method to be added to the many already known. While no single analytical method can solve all problems, and each element in each matrix needs separate thought, the following may be suggested as advantages of this method:

1. Sensitivity to ppb for many elements. Macro analyses also possible.

2. Ultimate accuracy, after development of sample-handling techniques for certain elements (such as oxygen and carbon), of 5%.

3. Only micro- to milligram samples are required.

4. Many elements can be analyzed simultaneously, and the "difficult elements," oxygen and carbon, are conveniently determined.

5. Analysis is non-destructive, but chemical separations may be done.

6. Interferences are limited, and can be removed or minimized by control of He^3 energy and selection of the detecting nuclear reaction and induced radioactivity. Positron emitters are generally produced allowing convenient detection of the 0.511-MeV annihilation radiation, either singly or in 0.511-0.511-MeV coincidence. Thus, gamma-ray spectra are simple, in contrast to the complex spectra observed in neutron activation analysis where computer "spectrum-stripping" techniques may be necessary.

7. The Coulomb barrier for the He^3 enables one to eliminate completely any radioactivities induced in the host or bulk material when analysis of a light element in a heavier host is desired, e.g., O^{16} in Au. This is a marked contrast to neutron activation analysis.

8. Charged-particle cross sections vary fairly smoothly with incident energy, and without drastic change from element to element, in contrast to neutron cross sections where large resonances from minute quantities of impurities can produce interfering amounts of induced radioactivities.

9. Analyses are rapid and can easily be automated for routine use.

10. The limited depth of penetration of a charge-particle beam is both an advantage and disadvantage depending on the goal. The use of a well-defined He^3 beam enables one to analyze surfaces, especially for the difficult elements oxygen and carbon. If, however, "bulk" analysis is desired, surface contamination is a distinct concern and sample-handling techniques in protective atmospheres may be necessary for certain elements. Simple glove-boxes, however, and placement of the sample in a covering envelope (such as Au foil) help to minimize this problem. The relative seriousness of the surface problem depends on the maximum He^3 energy available, and on what one defines as the "surface" depth.

What might be considered a "disadvantage" is a point shared by many forms of analysis, namely, the need for a particular piece of apparatus. Examples in "conventional" analyses of moderately elaborate and costly devices are mass spectrometers, X-ray machines, electron microprobes, emission spectrograph, and nuclear magnetic resonance analyzers.

In activation analysis by thermal neutrons, one usually employs a nuclear reactor, a complex and very costly device. For activation analysis by fast neutrons, the small 150 keV deuteron accelerators that produce 14-MeV neutrons by the d,t reaction are available at "moderate" cost.

For the He^3 activation analysis described herein, the Berkeley Hilac was used which gave 31-MeV He^3 ions. Such a large machine, however, is not necessary. The very favorable nuclear Q-values enable many of the detecting reactions to be induced with low-energy beams, i.e., 4 to 16 MeV. We thus suggest the development of a small, simple cyclotron designed especially for He^3 acceleration up to energies of about 16 MeV. Such a machine should be comparable, if not lower, in cost than some of the devices mentioned above. It should have an extracted beam of about 10 microamperes of He^3 (++), but 100 μA is certainly possible. A fixed-field cyclotron at 13 Mc and 15 kilogauss field would give 16 MeV He^3 (++) at a radius of only 13 inches, similar to the cyclotron previously suggested.[41]

It is calculated that 100 μA of He^3 at about 10-MeV incident energy on 9 mg/cm^2 of Be would also produce about 10^{11} [illegible] n/sec of energy 13 MeV. The reaction is $Be^9(He^3,n)C^{11}$ whose Q-value is +7.6 MeV. These neutrons would be emitted mainly in the forward direction and thus useful for fast-neutron activation analysis. Upon thermalization in paraffin, thermal-neutron activation analysis would be available. Neutrons of different energy would be readily obtained by variation of the target (the Q-value) and/or the energy of the He^3 beam.

?

The use of such a small cyclotron to accelerate other particles, such as protons, deuterons, and alphas, is also a possibility. Further, the acceleration of He^3, even to low kinetic energies, enables production of neutron-deficient nuclides, many of which are positron emitters difficult to produce by other cyclotrons. Such nuclides are of interest for nuclear spectroscopic studies and, in some cases, medical research projects.

ACKNOWLEDGMENTS

With pleasure and gratitude I acknowledge the assistance, support, and friendship of my research director, Professor Samuel S. Markowitz.

I am grateful to S. B. Hingorani, Bahman Parsa, Mary Reed, Jere Green, and Gil Butler for their cooperation and help in various aspects of my research.

The discussions and advice, often scientific, as well as the friendship of Dr. Paul Croft, Dr. John Olmsted, III, Dr. Arthur Pape, Dr. Edmond Roelof, and Dr. Charles Smith is deeply appreciated.

I should also like to acknowledge the help of David Anderson, Barbara Bailey, Dr. Lee Hyder, Dr. Paul Reeder, and Dr. David Seegmiller. I thank Chet Hatch, J. B. Johnston, Wilfred Kimlinger, Don Lebec, Jay Weidenfeld, and, posthumously, Sam Presley, as well as the other members of the Hilac crews who have assisted me with my experiments. The cooperation of the electronics support group, especially of Charles Campbell, in keeping the counting equipment operational is gratefully acknowledged.

I am very grateful to Carl Quong, who saved me considerable time by suggesting and writing the LENIC program. I also wish to acknowledge the assistance of the Chemistry Office staff whose cooperation in many ways, but especially near forgotten deadlines, is sincerely appreciated.

Finally, I wish to acknowledge and thank the people of Sacred Heart Parish, Oakland, California and of the Diocese of St. Augustine, Florida for their support during my four and one-half years here.

This work was performed under the auspices of the United States Atomic Energy Commission.

APPENDIX A

The Half-Life of F^{18}

A new, accurate, value for the half-life of F^{18} has been determined by Markowitz and the author.[82] The substantial amount of data available from the determination of the excitation function for the production of F^{18} from O^{16}, using He^3 as the incident particle, and additional half-life data taken on F^{18} from neutron and alpha reactions, were used.

Mylar was the oxygen source in the He^3 bombardments, Li_2SO_4, in the alpha-particle bombardments, and LiOH in the neutron activations. Chemical separations were used to isolate the F^{18} in the latter two procedures.

End-window proportional counting of the positrons was used; as a control, annihilation radiation emitted by one of the samples was counted with a NaI(Tl) scintillation counter and 256-channel pulse height analyzer.

The half-life was determined by means of the FRENIC[80] program which yields a value for λ as well as its standard deviation. The results of 10 individual experiments which met the "F" test[83] for consistency at the 95% confidence level were included in the calculation. The results of this research gave, for the weighted mean half-life[83] of F^{18} and the weighted standard deviation of the mean,[83] 109.72 ± 0.06 min.

APPENDIX B

The Excitation Function for Production of F^{18} from He^4 Reactions with O^{16}

In order to compare the cross section and thresholds for the reaction of He^3 particles with the reaction of He^4 particles with O^{16} to produce F^{18}, the excitation function for the production of F^{18} from He^4 reactions with O^{16} was determined. Exactly the same procedures as in the He^3 experiments were employed. Stacked Mylar foils were bombarded at the Hilac with 41.6-MeV α-particles. The F^{18} produced was counted by means of conventional end window β-proportional counters. Our results are shown in Fig. 11; those reported by Furukawa and Tanaka[84] are indicated by the broken line. The discrepancy between these results may be due to the difference in the range-energy relations used.

The principal reactions contributing to the production of F^{18} from O^{16} are (α,np), (α,d), and $(\alpha,2n)Ne^{18} \xrightarrow[1.5\text{ sec}]{\beta^+} F^{18}$; the thresholds for these reactions are, respectively, 20.4, 23.2, and 29.3 MeV in the laboratory system. It can be seen from Fig. 11 that 36 MeV α particles are required to reach the maximum F^{18} production cross section of only 150 mb, whereas a maximum cross section, 400 mb, for the He^3 reaction with O^{16} is reached at only 7.5 MeV (Fig. 3). Thus only a small accelerator would be required for practical He^3 activation analysis rather than the large (60-inch diameter) cyclotron needed for 40 MeV alpha particles.

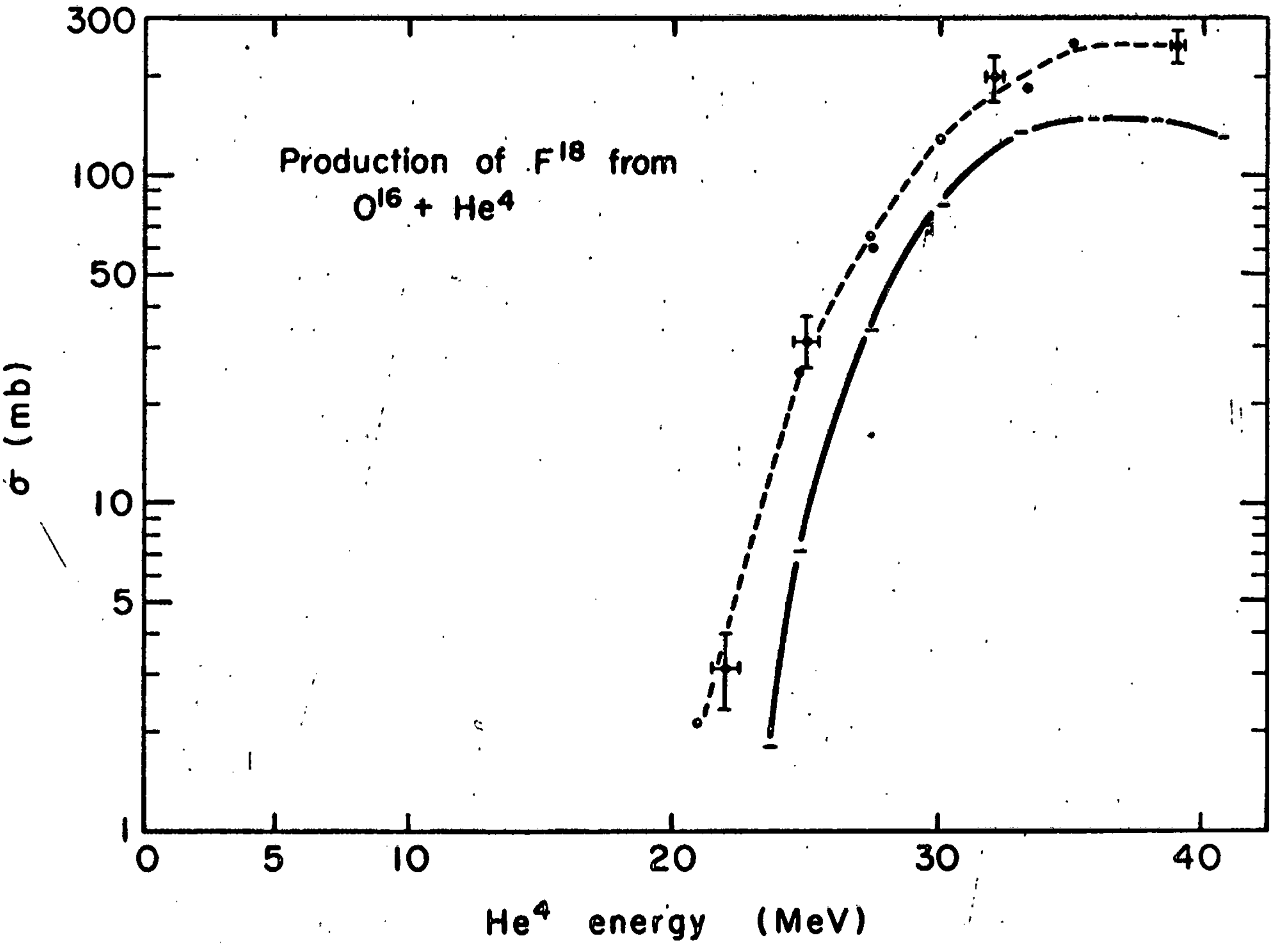

MUB-4613

Fig. 11. Excitation function for production of F^{18} from O^{16} by (α, np) + (α, d) + (α, 2n) reactions.

APPENDIX C

Summary of Overall Detection Coefficients and Resolving Time Corrections

The following tables give the overall detection coefficients for F^{18} and C^{11} for the end-window β-proportional counters used in the foregoing work. These efficiencies are normalized to a Cl^{35} standard (no. 2) which had a counting rate of 63,300 counts/min on shelf 3. The 4π standard, U^{238}, had a counting rate of 35,000 count/min. The ODC is simply the counting rate divided by the disintegration rate. The disintegration rate was calculated from the 4π counting rate and the positron branching of 97%[54] and 99.8%[87] for F^{18} and C^{11}, respectively.

Table I. Overall detection coefficients: counters A, B, C, D, E.

Fluorine-18 (0.65-MeV β^+ maximum)		Carbon-11 (0.95-MeV β^+ maximum)	
Shelf	ODC	Shelf	ODC
1	0.433	1	-
2	0.322	2	-
3	0.228	3	-
4	0.123	4	0.136
5	0.0734	5	-
6	0.0476	6	0.0538
7	0.0238	7	-
8	0.0141	8	-
9	0.0093	9	-

The variation of ODC among the counters is less than 2%. The value obtained for shelf 1 with F^{18} accurately conforms to that obtained by Reeder[88] using the method of Baghurst and Prestwood.[89]

Table II.

Resolving Times

Counter:	A	B	C	D	E	4π
Resolving time (μ sec):	6.9	8.4	14	5.6	11.3	30

Correction Factors*

Observed counting rate (counts/min)	A	B	C	D	E	4π
10^4	1.001	1.001	1.002	1.001	1.002	1.005
2×10^4	1.002	1.003	1.005	1.002	1.004	1.010
5×10^4	1.006	1.007	1.012	1.005	1.010	1.026
10^5	1.012	1.014	1.024	1.009	1.019	1.053
2×10^5	1.024	1.029	1.050	1.019	1.039	1.11
5×10^5	1.062	1.075	1.13	1.050	1.104	1.33
10^6	1.13	1.16	1.30	1.10	1.232	2.0

---

*The correction factor is that number by which the observed counting rate is multiplied to obtain the true counting rate.

REFERENCES

1. L. W. Alvarez and R. Cornog, Phys. Rev. 56, 379 (1939); 56, 613 (1939).
2. W. H. Barkos, Phys. Rev. 56, 1242 (1939).
3. D. A. Bromley and E. Almquist, He^3 Induced Nuclear Reactions, Atomic Energy of Canada, Ltd, Chalk River, Ontario, 1959.
4. S. S. Markowitz and J. M. Hall, Bull. Am. Phys. Soc. 4, 8 (1959).
5. G. Hevesy and H. Levi, Kgl. Danske Videnskab. Selskab, Mat.-Fys. Medd. 14, No. 5 (1936).
6. G. T. Seaborg and J. J. Livingood, J. Am. Chem. Soc. 60, 1784 (1938).
7. G. E. Boyd, Anal. Chem. 21, 335 (1949).
8. T. I. Taylor and W. W. Havens, Jr., Nucleonics 6, 54 (1950).
9. C. L. Gordon, Anal. Chem. 23, 81 (1951).
10. G. W. Leddicotte and S. A. Reynolds, Nucleonics 8, 62 (1951).
11. W. A. Brooksbank, G. W Leddicotte, and H. A. Mahlman, J. Phys. Chem. 57, 815 (1953).
12. C. L. Gordon, Anal. Chem. 26, 176 (1954).
13. J. A. Miskel and A. C. Wahl, Phys. Rev. 84, 700 (1951).
14. R. C. Plumb and J. E. Lewis, Nucleonics 13, 42 (1955).
15. W. A. Brooksbank and G. W. Leddicotte, J. Phys. Chem. 57, 819 (1953).
16. R. E. Connally and M. B. LeBoeuf, Anal. Chem. 25, 1095 (1953).
17. A. Moljk, R. W. P. Drever, and S. C. Curran, Nucleonics 13, 44 (1955).
18. G. E. Leddicotte and S. A. Reynolds, U.S.A.E.C. Report No. CF 56-7-106 (1956).
19. E. N. Jenkins and A. A. Smales, Quart. Rev. (London) 10, 83 (1956).
20. T. I. Taylor and W. W. Havens, Jr., Berl's Physical Methods in Chemical Analysis (Academic Press, New York, 1956), Vol. 3, p. 539.
21. W. W. Meinke, Anal. Chem. 28, 736 (1956).
22. W. W. Meinke, Anal. Chem. 30, 686 (1958).
23. D. Gibbons, B. A. Loveridge, and R. J. Millett, Brit. Atomic Energy Research Establishment Report No. AERE-I/R-2208 (1957).
24. R. C. Koch, Activation Analysis Handbook (Academic Press, New York, 1960).

25. H. J. M. Bowen and D. Gibbons, *Radioactivation Analysis* (Oxford University Press, London, 1963).

26. P. Albert, *L'analyse par radioactivation* (Gauthier-Villars and Cie, Paris, 1964).

27. B. M. Abraham, H. E. Flotow, and R. D. Carlson, Anal. Chem. 29, 1058 (1957).

28. S. Rubin, T. O. Passell, and L. E. Bailey, Anal. Chem. 29, 736 (1957).

29. E. Odeblad, Acta Radiol. 45, 396 (1956).

30. L. C. Bate, Nucleonics 21, 72 (1963).

31. P. Leveque, Proc. Intern. Conf. on the Peaceful Uses of Atomic Energy, U. N., New York, Vol. XV, Paper 342.

32. P. Süe, Compt. rend. 237, 1696 (1953).

33. E. Odeblad, Acta Radiol. 42, 391 (1954).

34. E. Odeblad and S. Odeblad, Anal. Chim. Acta 15, 114 (1956).

35. P. Albert, G. Chaudron, and P. Süe, Bull. Soc. Chim. France 20, C97 (1953).

36. P. Süe, Compt. rend. 242, 770 (1956).

37. B. L. Cohen, E. Newman, and T. H. Handley, Phys. Rev. 99, 723 (1955).

38. I. Fogelstrom-Fineman, O. Holm-Hansen, B. M. Tolbert, and M. Calvin, Intern. J. Appl. Radiation Isotopes 2, 280 (1957).

39. R. G. Osmond and A. A. Smales, Anal. Chim. Acta 10, 117 (1954).

40. B. A. Thompson, Anal. Chem. 33, 583 (1961).

41. S. S. Markowitz and J. D. Mahony, Anal. Chem. 34, 329 (1962).

42. R. C. Koch, *op. cit.*, p. 1.

43. E. L. Hubbard, W. R. Baker, K. W. Ehlers, et al., Rev. Sci. Instr. 32, 621 (1961).

44. G. Friedlander and J. W. Kennedy, *Nuclear and Radiochemistry* (John Wiley and Sons, Inc., New York, 1957), p. 194.

45. M. Rich and R. Madey, University of California Lawrence Radiation Laboratory Report UCRL-2301, March 1954.

46. J. H. Smith, Phys. Rev. 11, 32 (1947).

47. W. Whaling, in *Handbuch der Physik*, (Springer-Verlag, Berlin, 1958), Vol. 34, p. 193

48. H. Bichsel, Phys. Rev. 112, 1089 (1958).

49. A. Demildt, University of California Lawrence Radiation Laboratory Report UCRL-10647, February 1963.

50. C. Williamson and J. P. Boujot, Centre d'Etudes Nucleaires de Saclay, Rept. CEA 2189.

51. B. V. Rybakov, Sov. Phys. J.E.T.P. 1, 435 (1955).

52. T. B. Marion, Nuclear Data Tables, Part 3, U. S. Atomic Energy Comm., 1960

53. G. Friedlander and J. W. Kennedy, op. cit., p. 191.

54. D. H. Strominger, J. M. Hollander and G. T. Seaborg, Rev. Mod. Phys. 30, 585 (1958).

55. B. D. Pate and L. Yaffe, Can. J. Chem. 33, 929 (1955).

56. H. D. Holmgren, Proceedings of the International School of Physics Enrico Fermi Course, XV, Varenna on Lake Como, ed. G. Racah (Academic Press, New York, 1962).

57. J. H. Towle and B. E. F. Macefield, Proc. Phys. Soc. 77, 399 (1961).

58. N. H. Gale, J. B. Garg, and K. Ramavataram, Nucl. Phys. 22, 504 (1961).

59. D. Eccleshall and M. J. L. Yates, U.K.A.E.A.-AWRE Report NR/p-7/61.

60. R. Middleton, International Symposium on Direct Interactions and Nuclear Reaction Mechanisms, Padus, ed. E. Clementel and C. Villi (Gordon and Breach Science Publ., New York, 1962).

61. S. Hinds and B. M. Hinds, Nucl. Phys. 48, 690 (1963).

62. D. R. F. Cochran and J. D. Knight, Phys. Rev. 128, 1281 (1962).

63. D. A. Bromley, J. A. Kuehner and E. Almquist, Nucl. Phys. 13, 1 (1959).

64. H. D. Holmgren, H. Bullock, and W. E. Kung, Phys. Rev. 106, 100 (1957).

65. H. D. Holmgren, E. Geer, R. L. Johnston, and E. A. Wolichi, Phys. Rev. 106, 102 (1957).

66. S. Hinds and R. Middleton, Proc. Phys. Soc. 75, 745 (1960).

67. I. J. Taylor, F. de S. Barros, P. D. Forsyth, A. A. Jaffe, and S. Ramavataram, Proc. Phys. Soc. 75, 772 (1960).

68 V. M. Pankratov and I. N. Serikov, J.E.T.P. 45, 910 (1963).

69. J. Aguilar, W. E. Burcham, J. B. A. England, A. Garcia, P. E. Hodgson, P. V. March, J. S. C. McKee, E. M. Masinger, and W. T. Toner, Proc. Roy. Soc. 257, 13 (1960).

70. A. Garcia, J. Kirk, J. B. A. England, and P. E. Hodgson, Nucl. Phys. 38, 372 (1962).

71. H. M. Sen Gupta, J. Rotblat, P. E. Hodgson, and J. B. A. England, Nucl. Phys. 38, 361 (1962).

72. J. R. Priest, D. J. Tendam, and E. Bleuler, Phys. Rev. 119, 1295 (1960).

73. H. E. Wegner and W. S. Hall, Phys. Rev. 119, 1654 (1960).

74. J. B. Cunning, A. M. Poskanzer, and J. Hudis, Phys. Rev. Letters 6, 484 (1961).

75. V. A. Ryan, J. L. Green, and E. H. Lowenhaupt, Lawrence Radiation Laboratory Report UCRL-11618, August 1964.

76. W. Kaiser, P. H. Keck, and C. F. Lange, Phys. Rev. 101, 1264 (1956).

77. M. Tanenbaum, Semiconductors, ed. N. B. Hannay (Reinhold, New York, 1959), pp. 113, 114.

78. K. Saito, T. Nozaki, S. Tanaka, M. Furukawa, and Hwasheng Cheng, Int. J. Appl. Rad. Isotope 14, 357 (1963); T. Nazaki, S. Tanaka, M. Furukawa, and K. Saito, Nature 190, 39 (1961).

79. A. C. Demildt, Anal. Chem. 35, 1228 (1963).

80. A. C. Demildt, University of California Lawrence Radiation Laboratory, private communication, 1962.

81. J. L. Green, University of California Lawrence Radiation Laboratory, private communication.

82. G. R. Keepin, T. R. Wimett, and R. K. Zeigler, J. Nucl. Energy 6, 1 (1957). Revised by R. W. Hoff and J. O. Rasmussen, Lawrence Radiation Laboratory, Berkeley, California.

83. H. Medicus, P. Preiswerk, and P. Sherrer, Helv. Phys. Acta 23, 299 (1950).

84. J. D. Mahony and S. S. Markowitz, J. Inorg. Nucl. Chem. 26, 907 (1964).

85. L. G. Parratt, Probability and Experimental Error (John Wiley and Sons, New York, 1961).
86. M. Furukawa and S. Tanaka, J. Phys. Soc. Japan 16, 129 (1961).
87. J. Scobie and G. M. Lewis, Phil. Mag. 2, 1089 (1957).
88. P. L. Reeder (Ph. D. Thesis), University of California Lawrence Radiation Laboratory Report UCRL-10351, 1962 (unpublished).
89. B. P. Baghurst and R. J. Prestwood, Nucleonics 17, 82 (1959).